
The DONUT Approach to Ensemble Combination Forecasting

Reducing Human Assumptions in Forecasting using Deep Learning and
Optimization

Authors:
Ankile, Lars Lien
Krane, Kjartan

Abstract

This paper presents an ensemble forecasting method that shows strong results on the M4 Competition dataset by decreasing feature and model selection assumptions, termed DONUT (DO Not UTilize human assumptions). Our assumption reductions, consisting mainly of auto-generated features and a more diverse model pool for the ensemble, significantly outperforms the statistical-feature-based ensemble method FFORMA by Montero-Manso et al. (2020).

Furthermore, we investigate feature extraction with a Long short-term memory Network (LSTM) Autoencoder and find that such features contain crucial information not captured by traditional statistical feature approaches. The ensemble weighting model uses both LSTM features and statistical features to combine the models accurately. Analysis of feature importance and interaction show a slight superiority for LSTM features over the statistical ones alone. Clustering analysis shows that different essential LSTM features are different from most statistical features and each other. We also find that increasing the solution space of the weighting model by augmenting the ensemble with new models is something the weighting model learns to use, explaining part of the accuracy gains.

Lastly, we present a formal ex-post-facto analysis of optimal combination and selection for ensembles, quantifying differences through linear optimization on the M4 dataset. We also include a short proof that model combination is superior to model selection, *a posteriori*.

Table of Contents

List of Figures	iii
List of Tables	v
1 Introduction	1
2 Literature on Forecasting	2
2.1 Forecasting Problem Definition and Accuracy Measurement	2
2.2 M4 Competition and Data	3
2.3 LSTM in forecasting	4
2.4 Ensemble Forecasting	5
2.5 Statistical forecasting models	6
2.5.1 Ordinary Least Squares	6
2.5.2 Ornstein-Uhlenbeck Process	7
2.5.3 Local and Global Trend Model	7
2.5.4 Quantile Regression	8
2.6 Artificial Neural Networks	9
2.6.1 The Basics of Artificial Neural Networks	9
2.6.2 Gradient Descent	9
2.6.3 Hyperparameter Tuning	10
2.6.4 Early Stopping	10
3 Methods	10
3.1 A Data-Driven Ensemble	10
3.2 Algorithm	11
3.3 Theoretical Best Forecast of Ensembles	12
3.4 Ensemble Building Heuristics	13
3.5 Model selection vs. model weighting theory	15
3.5.1 Optimal Loss of Model Combinations and Selections	15
3.5.2 Computational proof of model weight ex-post superiority	16
3.6 Recurrent Autoencoder	16
3.7 LSTM Autoencoder Interpretation	18
3.7.1 Reconstruction Results and Interpretation	18
3.7.2 Measuring Importance of Features Generated by the Autoencoder	19
3.8 Automated Hyperparameter Search	20

3.9	Weight model	20
4	Results	21
4.1	M4 Test Data Forecasting Results	21
4.2	Performance Comparison to FFORMA model	23
4.3	Feature-Importance Results	24
4.4	Comparison to FFORMA in input space	28
5	Discussion	33
5.1	Reflections on the Results	33
5.2	Further Work	34
6	Conclusion	35
Bibliography		36
Appendix		38
A	Analysis of the Inner Workings of the LSTM Autoencoder	38
B	The M4 Competition Dataset of 100 000 Time Series	39
C	Feature and Loss Heat-maps	40

List of Figures

1	Overfitting Illustration	11
2	Model schematic. Hyper parameter search is used to decide the the meta variables of the model, marked in blue.	11
3	This is a plot where the optimal linear program solution clearly uses many forecasts and is successful. It is however not possible for the weight net to achieve a better result than 0.3 MASE given \mathcal{M}_{14}	13
4	A optimal forecast where the linear program solution is no where near the actual times series. Furthermore, just a single forecast was used, implying that all other methods were even further from ground truth.	14
5	A display of the ex post facto best weight of the models in our 14 ensembles on our validation set. To the left is a display of mean weights for all models. Our newly implemented models are given a relatively low weight ex post facto. The right figure shows that 2-3 models ensemble is the most common combination. 4 models and more add up to around 20% of all ensembles.	14
6	A display of the ex post facto best weight of the models of FFORMA on our validation set. To the left is a display of mean weights for all models. The right figure shows that 1-2 models ensemble is most common combination. 4 models our more adds up to around 7% of total optimal solution.	15
7	Greedy search for optimal ex post facto ensemble	15

8	The LSTM model architecture. There is two LSTM layers on each side of a bottleneck. There is also a dropout layer between the two LSTMs in the encoder.	17
9	Two different noisy sine-waves and their reconstructions. The noise is clearly filtered out and only the smooth sine-waves remain. The embedding dim used to represent recreate the sine curve is of length 4, while there are 100 time steps, ergo the recreation must be based on a compressed abstraction of sine	18
10	Original and reconstructed time-series from the M4 dataset of the validation partition, i.e. out-sample data. The autoencoder is able reconstruct many different types of time-series of different lengths, only based on a feature vector of length 32.	19
11	This figure depicts how the Autoencoder reacts to increasing noise. We generate a tanh function of 2000 data points. Then, iteratively, more and more random noise is added to it before it is given to the Autoencoder for reconstruction. The reconstruction is solid at minimal noise, shown with the purple line. The reconstruction has broken down at the other end of the spectrum, shown with the red line. This breakdown happens at around $2-3\sigma$ for the noise generation process or a signal-to-noise ratio of ca. 0.35.	19
12	Hyperparameter search graph	20
13	Left, the actual value compared to the forecast for a successful forecast. Right, the weights assigned to each model in the forecast on the left.	22
14	Left, the actual value compared to the forecast for a successful forecast. Right, the weights assigned to each model in the forecast on the left.	23
15	Left, a bar chart summarizing the mean weight each separate forecasting model was assigned by DONUT Fanciful over the entire test set. Right, the percentage of series for which DONUT Fanciful uses ensembles of a given size.	23
16	Colored boxes has p-value < 0.05, $\mu_0 = \text{mean}(\text{row}_{\text{box}})$: Our fanciful model has a mean OWA of 0.068 less than FFORMA for daily financial series, $n=1,559$. FFORMA relatively strongest in the demographic, weekly category but this has $n=24$	24
17	A visual representation of the feature importances for the 76 features our model uses. The features are listed in decreasing importance along the positive y-axis and x-values gives the deviation in OWA from the baseline when that feature is randomly permuted. The features generated by our Autoencoder are blue and the statistical features by Montero-Manso et al. (2020) are red. Several LSTM Autoencoder features have a high importance.	25
18	Hierarchical clustering of the correlation between all 76 features according to the ward's linkage. There is formed six distinct clusters of features. There is furthermore a tendency towards clustering among the statistical features and among the LSTM features.	26
19	A plot showing the permutation importances (perm. imp.) when scrambling (1) all features in the different clusters defined in Figure 18, (2) both meta variables alone (type, period), all statistical features alone, and all lstm features alone, and (3) all features that are not the meta variables (type, period), from left to right, respectively.	27
20	p -value < 0.05: A strong seasonal strength correlates with a low OWA, as indicated by a strong blue color. The Demographic series seems to be most easily predicted when seasonal_strength increases.	29
21	p - value < 0.05: Garch_r2, a measure of homoskedastic variance, also clearly correlates with a reasonable behavior from Fanciful sweep. Note how as the volatility measure increases, so does the difficulty of predicting, as indicated by a red color.	29

22	$p - value < 0.05$: Shows how lstm_6 also correlates with predictability. As lstm_6 increases all of the series seem easier to predict. The Autoencoder have provided information which correlates with a decrease in loss	30
23	$p - value < 0.05$: When plotting lstm_31 against seasonal strength, again it seems like the auto generated feature offers extra predictive power to our net compared to FFORMA, as seasonality decreases. Note how the top right corner, has a OWA decrease of .86, with $p < 0.05$	31
24	$p - value < 0.05$: When both lstm_31 and lstm_14 take on values near their medians, the DONUT mode does better than its average by a significant. This particular combination seem to elicit a non-linear relationship between the variables.	31
25	Synthetic data-set created to test noise filtering and clustering on increasingly difficult examples. The data is comprised of several copies of two different sines with different frequencies, and several Taylor approximations to one of them. All have considerable random noise added to them.	38
26	The six ways to slice the 4-dimensional space of one version of the trained autoencoder. The network is trained on M4 data, and the encoder is given the sines and Taylor approximations, and the raw outputs are plotted.	38
27	The distribution of different series lengths per series periodicity.	39
28	Cumulative number of time-series for series with for length to the value or shorter. By limiting the longest time-series to be 4 000, one in effect truncates less than 1% of all time-series, but saves more than half the storage space in memory while working with the data.	39
29	$p - value < 0.05$: When both lstm_31 and lstm_6 is low, or model beats Montero-Manso et al. (2020) by a significant margin. A decreasing linear combination between the two features seems to be positive for our weight nets predictive power.	40
30	$p - value < 0.05$: lstm_9 also shows a clear tendency of reducing error, over all types. 40	40
31	$p - value < 0.05$: Shows that when seasonality is low, has a decreased loss compared to Montero-Manso et al. (2020) by around .02 OWA. Such a loss reduction over all series is enough to move from a second to 6th place in the m4 competition.	41

List of Tables

1	An overview of the time series in the M4 dataset, as presented by Makridakis et al. (2018)	3
2	M-Competitions Summary	5
3	Table of the ex post facto MASE score for optimal model selection and optimal model combination for the FFORMA ensemble of nine models.	16
4	LSTM Autoencoder Hyperparameters	17
5	The hyperparameters for our final weight model, the model is a fully connected neural network.	20
6	Summary of our results compared to other relevant methods on the M4 dataset. Our method achieves a significantly better OWA result than the M4 second place, and a MASE better than both the first place and second place. [†] DONUT model did not enter competition but the rank is included to contextualize the result.	21

7	OWA loss for the method on the test set and for each subset of the data. Main finding is a OWA loss of 0.830, significantly better than Montero-Manso et al. (2020). Significance levels: $^*\alpha = 0.05$, $^{**}\alpha = 0.01$, and $^{***}\alpha = 0.001$	22
8	OWA improvement from FFORMA, with t-statistic and one sided p-value with $H_0 =$ FFORMA mean	24
9	Table summarizing the feature importances found for the trained weighting network with corresponding t -statistics and p -values. Significance levels: $^*\alpha = 0.05$, $^{**}\alpha = 0.01$, and $^{***}\alpha = 0.001$	32

1 Introduction

This paper investigates ensemble methods for forecasting, meaning the combination of simple method forecasts to improve accuracy and generalizability. We present the DO Not Utilize Human Assumptions (DONUT) method for ensemble combination forecasting. Our main contribution is to reduce assumptions for forecasting using time series features created from a Long Short-Term Memory (LSTM) Neural Network (NN) as inputs to a weighting of 14 statistical forecasting models. We also present an ex-post-facto analysis on optimal ensembles and provide a theoretical framework for ensembles of different flavors. This work has two central hypotheses:

Hypothesis 1: Fewer assumptions leads to better results.

It is possible to improve forecasting approaches by reducing human time-series assumptions in feature selection and weighting of the ensemble. In addition, large sets of data make learning and fitting hard forecasting problems possible.

Hypothesis 2: Machine learning methods can find relationships that humans are not able to uncover.

Machine learning methods can find features that contain richly descriptive qualities of a time series that are not necessarily linear, which traditional statistical measures cannot. Thus sets of statistical and machine-learned features can complement each other.

Less centrally to this paper but still of academic interest, we hypothesize that different series exert different levels of forecastability. In particular, we hypothesize that Demographic, Industry, and Macro series are more easily forecast than Finance and Micro, here termed the hypothesis of type. Furthermore, we believe ex-ante that low-frequency data is more easily forecast than high-frequency, since low-frequency data aggregate over more data and thus could be less susceptible to noise, here termed the hypothesis of sampling frequency.

In addition to exploring the hypotheses stated above, we have a two-fold goal in this paper. First, (1) to interpret the results from the best-performing models and understand what features of the time-series and models are essential for creating robust ensembles and accurate forecasts, thus separating reasonable assumptions from unproductive ones. Second, (2) to improve upon the results in the M4 competition by augmenting the methods and approaches that achieved the best results.

We start with a brief primer on the development of forecasting. The first studies conducted to assess the quality and accuracy of forecasting methods were conducted in the early seventies by Reid, Newbold, and Granger (Makridakis & Hibon, 2000; Newbold & Granger, 1974; Reid, 1969). Already in 1974, Newbold and Granger found that combining naïve forecasting methods in most cases produces better results than each of the methods individually (Newbold & Granger, 1974). This finding has been supported several times, e.g., in forecasting competitions and benchmarks like M1, M2, M3, where the complex methods did not outperform the more straightforward methods (Makridakis et al., 1982; Makridakis & Hibon, 2000). Many other researchers further corroborate these findings as well (Armstrong & Collopy, 1992; Fildes et al., 1998).

Analysis of the methods used in the M2 competition found that the simple average over the models in an ensemble outperformed a weighted average based on the in-sample covariance matrix of fitting errors, though this method also outperformed the individual methods Makridakis et al., 1982. This finding would indicate that when creating weighted averages, one must avoid over-fitting to the in-sample. Nevertheless, in the fourth Makridakis competition, M4, the top six methods significantly outperformed the simple ensemble benchmarks, albeit at a much higher computational cost (Makridakis et al., 2020), showing that the field has progressed. All of these methods except one use ensembles. Furthermore, the top two methods utilize modern machine learning (ML) techniques to some degree, an uplifting observation, as it shows that there are advances to be made within forecasting and that with better methods and more computing power, people can be better able to model the future and plan and make vital decisions accordingly.

The investigations resulted in a novel framework for forecasting using model combination en-

sembles, termed the *DONUT Approach*, short for DO Not Utilize Human Assumptions, that reduce the amount of judgment needed about the nature of the problem and data while producing accurate forecasts. First, in Section 2, we present some relevant theory underlying our model and related papers on which we draw. Next, in Section 3, we present several of the methods we use in-depth, as well as an analysis of the dynamics of optimal ensembles. Then, in Section 4, we present the most compelling results from the DONUT model, including analyses of the performance compared to Montero-Manso et al. (2020) and analysis of the features created by the autoencoder. Finally, in Section 5, we reflect upon the results and some implications before we shed light upon where we believe we can find further performance enhancements.

2 Literature on Forecasting

This section presents the relevant theory underlying our model and the related papers laying the foundation for this work. First, we discuss the forecasting problem and loss functions. In the M competition of which we draw many ideas and data. Then we discuss the usage of LSTMs in forecasting and some theoretical work on ensemble forecasting. Lastly, we describe the models we have added to our final ensemble and theory on Neural Networks, of which our weighting model is an example.

2.1 Forecasting Problem Definition and Accuracy Measurement

In this paper, we work with the problem of univariate point forecasts for time series (TS) in discrete time. The problem of univariate forecasting is as follows: Given a forecast horizon h and a set of observed previous values of the TS $\mathbf{y}_t = [y_1, \dots, y_t] \in \mathbb{R}^T$ of length t , produce a vector of forecasts of length h $\hat{\mathbf{y}}_{t+h} = [\hat{y}_{t+1}, \dots, \hat{y}_{t+h}] \in \mathbb{R}^h$ that is “similar” to $\mathbf{y}_{t+h} = [y_{t+1}, \dots, y_{t+h}] \in \mathbb{R}^h$. A forecasting model has the form

$$f(\mathbf{y}_t; \theta, \mathcal{M}) = \hat{\mathbf{y}}_{t+h}, \quad (1)$$

where θ is the model parameters and \mathcal{M} is the set of available models in the ensemble model, described in detail in Section 2.4.

To assess the performance of a system or a model, one needs a way to quantify the “similar” property, which is a function from $\hat{\mathbf{y}}_t$ mapped to how well or badly one does on unseen data. If this function is defined neatly, one can optimize it by tweaking the parameters of f . The objective function or criterion is the function we want to minimize or maximize. When the goal is to minimize an objective function, it is usually connote as a *loss function*, as it is a measure of the badness of fit, i.e., error or loss. To optimize a model efficiently, an important feature of a loss function is it being continuous so that small changes to the parameters translate into a small change in the loss, facilitating optimization through, e.g., gradient descent. Furthermore, as the loss function will represent how “good” a model is, it is vital that it truly represents the overarching goals of the model (Reed & MarksII, 1999). Let \mathcal{L} be any loss function that exists in the set of possible loss functions \mathcal{L}_Ω . A loss function for our problem will take the following form,

$$\mathcal{L}(\mathbf{y}_{t+h}, \hat{\mathbf{y}}_{t+h}) \in \mathbb{R}. \quad (2)$$

We have opted to use the same loss functions employed in the M4 Competition during the fitting and testing of our model: Overall OWA, sMAPE, and MASE. First and foremost, this allows us to compare our performance to the performance of the models in the Competition. Moreover, the loss functions have the property of being continuous, as mentioned as necessary above. Lastly, the measures allow for comparing across TS of different levels, unlike, e.g., the mean absolute error (Hyndman & Athanasopoulos, 2018). The primary measure is the OWA loss function as described

	Micro	Industry	Macro	Finance	Demographic	Other	Total
Yearly	6538	3716	3903	6519	1088	1236	23000
Quarterly	6020	4637	5315	5305	1858	865	24000
Monthly	10975	10017	10016	10987	5728	277	48000
Weekly	112	6	41	164	24	12	359
Daily	1476	422	127	1559	10	633	4227
Hourly	0	0	0	0	0	414	414
Total	25121	18798	19402	24534	8708	3437	100000

Table 1: An overview of the time series in the M4 dataset, as presented by Makridakis et al. (2018)

by Makridakis et al. (2018), see Equation 5. The OWA loss function is a normalized combination of sMAPE and MASE, two standard accuracy measures used in the field of forecasting (Petropoulos et al., 2020). Both sMAPE and MASE are based on an absolute difference between actual and forecast but differ in how they normalize the sum difference. Both are defined below.

$$\text{sMAPE} = \frac{2}{h} \sum_{t=n+1}^{n+h} \frac{|Y_t - \hat{Y}_t|}{|Y_t| + |\hat{Y}_t|} * 100\% \quad (3)$$

$$\text{MASE} = \frac{1}{h} \frac{\sum_{t=n+1}^{n+h} |Y_t - \hat{Y}_t|}{\frac{1}{n-m} \sum_{t=m+1}^n |Y_t| - |Y_{t-m}|} \quad (4)$$

$$\text{OWA} = \frac{1}{2} \left[\frac{\text{sMAPE}}{\text{sMAPE}_{\text{Naïve2}}} + \frac{\text{MASE}}{\text{MASE}_{\text{Naïve2}}} \right] \quad (5)$$

There are, of course, several other loss measures for time series accuracy. Mean Absolute Error (MAE) and Mean Squared Error (MSE) is perhaps the most simple and pervasive. However, we did not use these since MAE is hard to compare across time series of different levels, and Armstrong and Collopy (1992) showed that MSE is unreliable for comparisons between series.

Through some algebraic manipulation, one can rewrite the MASE loss as the objective function of a linear optimization program. Thus one can expect a posteriori to find a global minimum MASE loss.

This paper uses “accuracy” as a term meaning reduction of a loss measure if the context does not imply otherwise.

2.2 M4 Competition and Data

This paper presents a model based on an extensive analysis of the findings of the Makridakis M4 forecasting competition (Makridakis et al., 2018). We have combined ideas, mainly from the two winning papers by Smyl (2020) and Montero-Manso et al. (2020), as well as augmenting the methods with our ideas and other methods from the literature. The M4 Competition hosted 248 contestants from 46 countries, of whom 49 teams provided valid forecasts for the 100,000 times series Makridakis et al., 2018.

Especially the top two papers of the M4 Competition have inspired our work, and specifically, we draw a lot from Montero-Manso et al. (2020) and their FFORMA model as it exploits the established finding that ensembles tend to outperform their constituent parts. Furthermore, the winning paper by Smyl (2020) and its hybrid solution discusses that using all information about a time series available (e.g., time-series type) is essential for accurate forecasts. Using information about a time series makes intuitive sense because different time series behave differently, like an interest rate or the demand for a specific widget.

This paper has made an ensemble forecasting technique by augmenting the FFORMA model in several ways. In Montero-Manso et al., 2020 the main idea is to use statistical features of a time series (e.g., trend, variance, seasonality) as inputs to a model that weights the output of 9 more straightforward forecasting methods. These models include the naïve forecast, ARIMA, exponential smoothing, and other established models. By weighting individual forecasts from simple models, the hope is that complex behavior may arise from simpler building blocks. In short, FFORMA produces 42 statistical features and nine forecasts for each of the 100,000 series. Then, they use the gradient tree boosting algorithm, XGBoost (Chen & Guestrin, 2016), combined with a custom loss function, to produce weights for the nine models based on the statistical features as inputs. Importantly, XGBoost does not forecast the actual time-series but rather a weighting of forecasting models. This method rests on the assumption that statistical features have predictive power for weighting an ensemble, which, given their result on the M4 data, seems to be supported. Then, they train the algorithm with a modified version of OWA as their loss measure. Its goal is to minimize the forecasting error the models produce if picked at random, using these probabilities as weights. The FFORMA model is thus trying to find the correct weights for each model and not choose the best model, like in a classification task. This last differentiation is akin to the dichotomy between model selection and model combination as discussed in Section 2.4.

Montero-Manso et al. (2020) find significant improvement from averaging over the models compared to picking the single best model. Furthermore, their OWA loss is 14% smaller than simple averaging across all nine models. This finding is compelling, as their ensemble approach has done better than the two extremes: (1) a single model and (2) simple averaging, contradicting the findings of Makridakis et al. (1982), showing that the field of forecasting has improved drastically since 1982.

We have collected their 9 model forecast and their statistical features for all 100,000 time series in this work. Basing the model on forecasts in a file somewhat reduces the flexibility of the approach, rather than being models we can refit for other purposes. Regardless, this approach fits this use-case well and forms the basis for which we build our model, and as we argue, reduce the assumptions made about model input and output. They have conveniently made their code available on GitHub: M4metalearning.

In Table 2 we have summarized the results from each of the previous M competitions, telling the story of how publicly available forecasting methods have improved over the years. A significant finding in the first three M-competitions was that more sophisticated methods generally did not outperform simple methods such as naïve and performed worse when the test series contained considerable noise. Furthermore, averaging multiple methods or combining them somehow proved more successful in the M1 and M3 competitions. Another interesting finding from the M2 Competition was that the most significant improvements in forecasting accuracy came from measuring and extrapolating the seasonality of a series. The findings marked with a dagger[†] in Table 2 are especially relevant for our approach.

Although both the M5 and M6 competitions are available, we decided not to forecast these newer datasets. The M5 Competition caters to a specific problem (predicting Wall-Mart sales), and M6 contains only financial time-series. Thus we thought the M4 competition data had a broader interest. The M6 Competition does not yet have any test results, leading to less compelling findings since any result would have to come from a held-out test set, which clouds any discoveries since comparisons with other models become difficult.

2.3 LSTM in forecasting

We chose to use Long Short Term Memory network (LSTM) in part due to the paper by Laptev et al. (2017) (winner of M4, Smly, is also co-author). The paper uses an LSTM for feature extraction, thus creating condensed inputs that will function as features for a neural network to make predictions. Furthermore, some statistical features are used in addition to the LSTM features, possibly giving the output even more predictive power. The authors developed new methods to predict extreme events in Uber’s data, e.g., a drastic reduction in traffic on Christmas Day. Compared to current univariate machine-learned models, they improve forecast accuracy by 2% - 18%. They also showed decent results on the M3 competition data, outperforming several

M1, 1982
<ul style="list-style-type: none"> • The accuracy measure utilized can change the ranking of the different methods • Performance of the various methods depend upon the length of the forecasting horizon • Accuracy of combinations of methods outperforms on average the single methods alone and does well in comparison with other methods • Given an ensemble of methods, the simple average over them outperformed the more complex average based on covariates, though that still did well
M2, 1993
<ul style="list-style-type: none"> • Good and robust performance of exponential smoothing methods. • Less randomness leads to better relative accuracy of the more sophisticated methods • The greatest improvement in forecasting accuracy came from measurement and extrapolating the seasonality of the series[†]
M3, 2000
<ul style="list-style-type: none"> • Statistical and sophisticated methods do not necessarily produce more accurate forecast than simple ones[†] • Accuracy of combinations of methods outperforms on average the single methods alone and does well in comparison with other methods[†]

Table 2: Summarized M competition findings. [†]The most relevant findings for this paper are marked with a dagger.

traditional methods indicating good generalization. They also use the R-forecasting package to collect statistical features, although an earlier version than what is available online as of the time of the submission of this paper, with only 15 features.

Laptev et al. (2017) find that a high number, long length, and existence of a correlation between time series indicate that NNs could be superior to statistical methods. However, statistical methods still seem to be superior in more straightforward cases. A resulting hypothesis is that using NNs to combine statistical models allows for the discovery of complex relationships given enough data and the possibility of weighting simple statistical models when the signal-to-noise ratio is low, or the number of series is small.

In our case, the most important result from this paper is the use of the LSTM. While Laptev et al. (2017) also uses an LSTM for forecasting, the idea of LSTM generated features is one of our core approaches.

2.4 Ensemble Forecasting

On a high level, there are two ways to produce forecasts. The first, and simplest, is using a single model, and the second is combining several models into a single forecast, referred to as an ensemble in literature (Montero-Manso et al., 2020). In a large body of research, ensemble methods are shown superior to single-model approaches, starting in 1969 with Bates and Granger (1969), further supported by many others (e.g. Clemen (1989), Makridakis and Hibon (2000) and Timmermann (2006)).

There are two main ways of producing ensemble forecasts given a set of forecasting methods, \mathcal{M} that all produce forecasts for the same Time Series (TS). (1) *Model selection* involves picking the most promising model $m \in \mathcal{M}$, based on limited information, that will have the highest accuracy. (2) *Model combination*, on the other hand, involves estimating weights for each forecast $\hat{\mathbf{p}}_{\mathcal{M}} = \{\hat{p}_m | \sum \hat{p}_m = 1 \wedge \hat{p}_m \geq 0\} \quad \forall m \in \mathcal{M}$, such that the accuracy of the weighted average is as high as possible. Generally, an aim is that the model combination outperforms the accuracy of the individual forecasts combined (Petropoulos et al., 2020). In this work, we focus on the combination of forecasting models, which will often be referred to as *model weighting*, as we, in effect, create weighted averages over the models.

Lemke and Gabrys (2010) found that combining forecasts improved the performance over the performance of the best individual predictors and thus showed that a combination strategy can

outperform a model selection one even on the meta-level. We also prove that this must mathematically be the case in the optimal ex-post case as well, in Section 3.5.1.

The “no-free-lunch” theorem establishes that no algorithm can outperform all other models or the random forecast when testing on all possible data (Wolpert, 1996). This theorem implies that without knowing anything about a problem, one cannot assume anything about the performance of an algorithm (Lemke & Gabrys, 2010). Of course, there will be specific problems for which one algorithm performs better than another in practice. Thus, Lemke and Gabrys (2010) shows that the above assumption can be relaxed by automatically extracting features from series that will function as a proxy for domain knowledge. Furthermore, Goodfellow et al. (2016) argues that the reason model combination works are that different models will not have residuals with perfect correlation for the test set. At the same time, model diversity alone must not be the only aspect of an accurate combination of methods—it is individual accuracy as well, according to Lemke and Gabrys (2010).

Lastly, an important reason for us to choose a model combination ensemble is the interpretability it offers. We thought it interesting to interpret the results and weights our weighting entity offered. On a personal note, since this is part of our master thesis, we needed to be left with results one could explain, independent of the actual test results.

2.5 Statistical forecasting models

In this section, we explain the workings of five models we have added to the existing nine models used by Montero-Manso et al. (2020), and some rationale for adding each model to the set of available models \mathcal{M} .

2.5.1 Ordinary Least Squares

Ordinary Least Squares (OLS) is a method that permeates the statistical landscape. First introduced by Gauss (1823), OLS is a method of minimizing the squared residuals between a dependent variable and a linear combination of independent variables. The Gauss-Markov theorem as presented in Greene (2018) states the following.

“In the linear regression model with given regressor matrix \mathbf{M} , (1) the least squares estimator \mathbf{b} is the minimum variance linear unbiased estimator of $\boldsymbol{\beta}$ and (2) for any vector of constants \mathbf{w} , the minimum variance linear unbiased estimator of $\mathbf{w}'\boldsymbol{\beta}$ is $\mathbf{w}'\mathbf{b}$.”

Greene (2018) presents five requirements for the OLS estimator to have the qualities of a Best, Linear, Unbiased Estimator (BLUE), a commonly desired property of an estimator. These are as follows. A1. The regression model is linear in its parameters. A2. There is a random sampling of observations. A3. A conditional mean of zero. A4. There is no multi-collinearity (or perfect collinearity). A5. Spherical errors: There is homoskedasticity and no auto-correlation.

Thus, we think that given that a time series follows the above properties and that there is a linear relationship between time (our independent variable in the case of the M4 univariate series) and the dependent variable, OLS could be an excellent model to add to our ensemble. Furthermore, since several of the statistical features we use tests for homoskedasticity, auto-correlation, and orders of integration, we stipulate that the neural net is provided the necessary information to weight OLS appropriately when these criteria take on values that allows OLS to be BLUE. For instance, the Kwiatkowski–Phillips–Schmidt–Shin test (KPSS), which tests for trend-stationary time series (Kwiatkowski et al., 1992), is one of the available features. Thus, the weighting model could utilize the linear model when the KPSS feature takes appropriate values. In principle, the model could then deploy OLS with reasonable confidence that the conditional mean of the error term is 0.

The OLS univariate linear regression-based model would perform well for a process y_t defined as

$$y_t = \alpha + \beta t + \epsilon_t, \quad (6)$$

where y_t is the value of the process, α a level term, β the linear relationship coefficient between the time t and the dependent variable, and ϵ_t is a normally distributed error term with mean 0. The literature defines a model estimating the process in Equation 7 as

$$\hat{y}_t = \hat{\alpha} + \hat{\beta}t, \quad (7)$$

$$\text{where } \hat{\beta} = \frac{n \sum t y_t - \sum t \sum y_t}{n \sum t^2 - (\sum t)^2}, \quad (8)$$

$$\text{and } \hat{\alpha} = \bar{y} - \hat{\beta} \bar{x}. \quad (9)$$

In the above, the hats above the parameters, e.g., $\hat{H} \alpha$, denotes estimated parameters. In a multivariate case, one could add more regressors and more advanced methods with dummy variables to model, e.g., seasonality and structural breaks. Other models in our ensemble try to utilize these more advanced forecasting techniques.

2.5.2 Ornstein-Uhlenbeck Process

An Ornstein-Uhlenbeck (OU) process is a stochastic differential model representing mean-reverting processes (Schöbel & Zhu, 1999). We define a simplified model for the dependent variable as

$$dS = \gamma(m - S)dt + \sigma dZ, \quad (10)$$

where S is the dependent variable, m is the time-independent mean, dt is the change in time and dZ is a Wiener process (Bibbona et al., 2008; Wiener, 1976). One often interprets γ as the reversion velocity, i.e., how fast the process returns to the steady-state once a shock or deviation occurs. One can analytically solve the above stochastic differential equation. However, it is more efficient to estimate it using numerical methods for computational approaches using the above model.

We chose to add the OU process as we thought it possible for the weighting model to identify mean-reverting time series, and the OU model will complement the existing models, cf. the discussion in Section 2.4. E.g., researchers often model commodity prices as mean-reverting processes, and there are both financial theory and empirical evidence for the existence of mean-reverting assets. For example, Bessembinder et al. (1995) finds that 44% of a typical spot oil price shock, in expectation, reverses over the following eight months. Contextualizing this, given that our task for monthly series is to predict 18 time-steps into the future, adding a mean-reverting process could account for such a shock given that the weighting model can identify some probability of mean reversion in a series. Furthermore, the financial theory argument is, in short, based on supply and demand, and the tendency of supply and demand to increase and decrease respectively at a higher price and thus shock adjusting prices (and vice versa for low price shock).

Commonly, practitioners find OU parameters by using the maximum likelihood method. We mention that we have adjusted σ in our final implementation since the Wiener Process explains the forecast S in the short term to a more considerable extent. However, it is desirable for the model to predict signal rather than noise, and have thus opted to reduce the noise in the Ornstein-Uhlenbeck process, as we stipulate that it will increase the speed of learning how to act if and when mean reversion occurs.

2.5.3 Local and Global Trend Model

The Local and Global Trend model (LGT) is perhaps the least known methods of the ones chosen to augment the ensemble. LGT, as presented by Ng et al. (2020), is a statistical forecasting model combining different time series attributes to generate forecasts,

$$y_t = \mu_t + s_t + \epsilon_t \quad (11)$$

$$\mu_t = l_{t-1} + \xi_1 b_{t-1} + \xi_2 l_{t-1}^\lambda \quad (12)$$

$$\epsilon \sim \text{Student}(0, v_0, \sigma) \quad (13)$$

$$\sigma \sim \text{Gauchy}(0, \gamma_0), \quad (14)$$

where $l_t, \xi_1 b_t, \xi_2 l_{t-1}^\lambda, s_t, \epsilon_t$ are modeling level, local trend, global trend, seasonality, and error term, respectively. γ_0 is a data driven scalar. As such, the model follows a triple exponential smoothing form in the updating process, which has proven effective in practical forecasting applications (Siregar et al., 2017).

The model is a state-space model and is thus part of the large body of work in this field (Ng et al., 2020). State-space models have in common that they try to explain a dependent variable by another state variable, of which it has its name. In literature, these are often called the measurement equation and the transition equation, where the first is the observed dependent variable while the other tracks the change or transition of the state (Brooks, 2019). In the specific example of LGT, Equation 12 and Equation 13 would be the measurement and transition equation, respectively.

The main reason for the addition of LGT is the promising results shown by Ng et al. (2020). Out of the models compared in the paper, LGT is the number one method for predicting M3 Competition data, significantly beating benchmarks such as sARIMA. On M4 weekly data, it underperforms compared to some methods but outperforms the remaining two other data sets analyzed in the paper. Another reason for the addition of LGT is that a state-space model seems plausible that some time series are well described. It would thus be interesting to analyze what weight, and in what situations such a model would be given weight, by the weighting model.

Lastly, a Python implementation of LGT is freely available in the GitHub package [Orbit](#), and as such, the model is efficiently implemented and added to the ensemble, despite being reasonably complex.

2.5.4 Quantile Regression

Quantile regression is a method that resembles the classic OLS regression, except for estimating the conditional median of the dependent variable instead of the mean (Brooks, 2019).

Quantile regression, first developed by Koenker and Bassett Jr (1978), offers a way of handling complex relationships between a dependent variable and regressors using conditional quantiles. For example, the median is less sensitive to outliers than the mean, and quantile regressions offer a more versatile distribution measure over possible values than standard OLS. Another strength is that it is non-parametric and does not make any assumptions about the variable distribution. Furthermore, we can adjust the model to forecast the quantiles τ in which we are interested.

Brooks (2019) defines quantile regression, for a given quantile τ , as a representation of the model to estimate $\hat{\beta}$ as

$$\hat{\beta} = \operatorname{argmin}_{\beta} \left(\beta \left(\sum_{i:y_i > \beta x_i}^N \tau |y_i - \beta x_i| + \sum_{i:y_i < \beta x_i}^N (1 - \tau) |y_i - \beta x_i| \right) \right) \quad (15)$$

$$Q(\tau) = \inf y : CD(y) \geq \tau, \quad (16)$$

where $CD(\cdot)$ is the cumulative distribution, and infimum is the greatest lower bound such that the inequality is satisfied. In our case, the regressor x_i is as in Equation 7 i.e. the time step t .

In our ensemble, \mathcal{M} , we have included quantile regressions the two values of τ , $\tau_{.99} = .99$ and $\tau_{.01} = 0.01$. We chose these levels for the quantile regressions to provide the weighting model with

a larger space of possible forecasts to choose from, again cf. the discussion of model diversity in Section 2.4. The $\tau_{.99}$ level regression provides the weighting model with the possibility of predicting steeper growth than any of the other models alone. The $\tau_{.01} = 0.01$ level regression, on the other hand, makes it possible to add hard dampening of the forecasted growth of a series. Both cases rely on the model learning a relationship between the input features and series where such increased or decreased growth is beneficial.

2.6 Artificial Neural Networks

2.6.1 The Basics of Artificial Neural Networks

An Artificial Neural Network (NN) is a subset of machine learning methods that are given their name by mimicking the human brain. In our full ensemble model, we use two NNs. One is the Fully Connected NN that produces the weights for the different forecasting models $m \in \mathcal{M}$, thus producing a prediction \hat{y}_{t+h} . The other is the Long Short-Term NN which extracts time-invariant features from the time series, which we discuss in more detail in Section 2.3).

A NN performs non-linear transformations from input to output and can, in theory, approximate any real-valued function from one finite-dimensional space to another to any desired degree of accuracy. Provided there is at least one hidden layer, a non-linear squashing function is present, and sufficiently many hidden units are available (Hornik et al., 1989). A NN works by iteratively using matrix multiplication (linear transformation), importantly followed by a non-linear function (Goodfellow et al., 2016). Equation 17 shows a single non-linear transformation layer \mathbf{L} , where g is a non-linear activation function, \mathbf{A} is a linear transformation, and \mathbf{b} is the bias. There is a difference in the complexity a linear, and non-linear model can learn, for instance, the XOR function, which is infeasible for a linear function but trivial for several non-linear models (Minsky & Papert, 2017).

$$\mathbf{L} = g(\mathbf{A}^T \mathbf{x} + \mathbf{b}) \quad (17)$$

One can depict a NN as a graph, and, more formally, it is the iterative application of the above function for an arbitrary number of steps, with an arbitrary number of parameters at each step (this flexibility makes the model susceptible to being over-parameterized, which we briefly discuss in Section 2.6.4). For instance a neural network with one hidden layer could be written as $y_{dep} = L_{out} \circ L_h \circ L_{in}(x_{ind})$. The first layer, the input layer, is provided data, which is passed through the network, layer by layer. At the last layer, L_{out} creates the output with a fitting activation that is application-specific (e.g., classification or regression). The output then flows to a loss measure (see Section 2.1), which updates the parameters in the network (often called weights), backward through the layers in a process called backpropagation (Goodfellow et al., 2016). Note that if one were to remove g from Equation 17, the complexity increase from iteratively adding layers would be removed as $\mathbf{A}_1 \mathbf{A}_2 \dots \mathbf{A}_n \mathbf{x} = \mathbf{A} \mathbf{x}$, results in a linear transformation, where \mathbf{A}_i are all linear transformations.

A Fully Connected Neural Network, as our weighting model is an example of, is an NN where all layers are fully connected, i.e., there is an edge between each node in one layer to all nodes in the next (nm connections between a layer with n and m nodes).

2.6.2 Gradient Descent

Gradient descent is a way of fitting NNs by reducing the value of $f(x)$ by moving a small negative direction of the derivative. Equation 18 shows how gradient descent is deduced as in Goodfellow et al. (2016). Since the relationship

$$f(x + \epsilon) \approx f(x) + \epsilon \frac{df}{dx}, \quad (18)$$

holds at sufficiently small ϵ , the derivative helps minimize a loss function as it shows what direction would cause a decrease in the loss (i.e., an increase in performance or accuracy). This observation leads to the relationship

$$\rightarrow f(x - \epsilon \cdot \text{sign}(\frac{df}{dx}))f(x), \quad (19)$$

for ϵ small enough. Therefore, we can minimize the loss by moving in small increments in the opposite direction of the derivative. Cauchy et al. (1847) originally termed this process gradient descent.

Gradient descent is the primary step of backpropagation, where each weight is updated recursively backward through the model, layer by layer. Gradient descent can also be generalized for multi-input cases, where the aim would be to move in the direction of the steepest descent in the multidimensional space of the loss function. In the multi-variable case, we would get

$$\theta' = \theta - \epsilon \nabla_{\theta} \mathcal{L}(\theta), \quad (20)$$

where ϵ is the learning rate and $\nabla_{\theta} \mathcal{L}(\theta)$ is the vector containing all partial derivatives of the loss function \mathcal{L} with respect to the model parameters θ (Goodfellow et al., 2016).

2.6.3 Hyperparameter Tuning

Modern machine learning models have increased exponentially in complexity over the last couple of decades, and with it, an exponentially increasing space of hyperparameters to search over Li et al., 2017. Unfortunately, there are, in general, no methods that guarantee optimal hyperparameters except for a brute force search, for most hyperparameters Snoek et al., 2012. We present a discussion about how we can solve this vital issue in Section 3.8.

2.6.4 Early Stopping

Large models with a sufficiently large number of parameters can suffer from overfitting, meaning that the model stops learning general relationships between input and output and instead learns to fit the noise of, or memorize, the training set. We can observe this phenomenon by a deviation in training and validation loss, exemplified in Figure 1 (Goodfellow et al., 2016). Goodfellow et al. (2016) argue that the best regularization technique for NNs is to stop the training at the point where the validation loss is at its lowest, known as *early stopping*. This regularization technique requires using some of the training data as a validation set, reducing the size of the training set. This limitation can be overcome by retraining on the entire training set using the exact specifications as found previously with the optimal hyperparameters and stopping point (Goodfellow et al., 2016).

3 Methods

In this section, we present the methods we have used in-depth and an analysis of the dynamics of optimal ensembles. We start by Presenting our data-driven ensemble algorithm top-down. We then present some forecasting theory and a model to understand how ensemble loss occurs.

3.1 A Data-Driven Ensemble

In several papers, we found a high degree of modeling decisions made based on a qualitative judgment rather than empirical and quantitative investigations. We suspect that such judgments

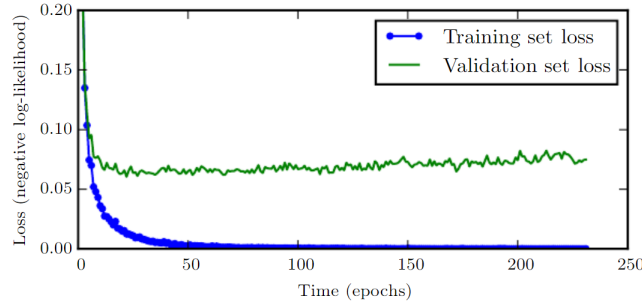


Figure 1: Illustration of the tell-tale signature of a model that has been overfitted. The defining factor is that the training loss falls (blue line) while the validation loss (green) starts to increase. (Source: Goodfellow et al., 2016)

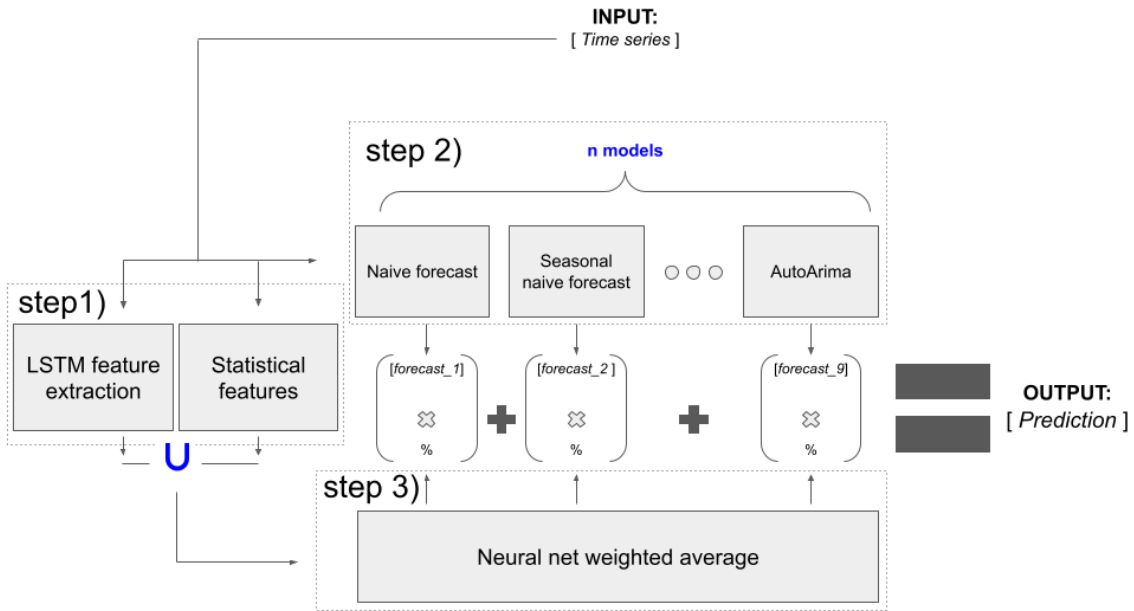


Figure 2: Model schematic. Hyper parameter search is used to decide the the meta variables of the model, marked in blue.

could lead to bias and erroneous assumptions. Therefore, we choose both the features used for combining statistical models and the statistical models used in the ensemble by quantitatively assessing their effectiveness, as described in Section 2.6.3.

3.2 Algorithm

Our algorithm consists of 3 main steps, enumerated in Figure 2. Furthermore, all or code is found in the GitHub repository: [krankile/ensemble_forecasting](https://github.com/krankile/ensemble_forecasting).

The following is a top-down view of how our algorithm work:

step 1 We fit a Long Short Term Memory model to the set of time series. Thereafter use the fitted model to create 32 novel features of the time series. We also collect statistical features based on the tsfeatures R library as found in Montero-Manso et al., 2020.

step 2) We create forecast based on 14 models, 9 of which are collected from FFORMA Montero-Manso et al., 2020. The full list of all the statistical models we use are as in FFORMA with addition of the following:

1. OLS
2. Ornstein Uhlenbeck Mean Reversion
3. Local and Global Trend Model (Ng et al., 2020)
4. .99 Quantile Regression
5. .01 Quantile Regression

step 3) We weight these forecasts based on the LSTM and statistical features, consisting of 74 features in total. We also use two meta-variables as inputs, the “Period”, which is the time delta of successive observations of a series, and “type”, according to the columns in Table 1. A weighting neural net is trained vs. actual values according to OWA loss. The results are then acquired from predicting the separate test set as provided in the M4 competition.

3.3 Theoretical Best Forecast of Ensembles

In this section, we shed some light on the theoretical best ensembles for a given \mathbf{y}_t , \mathcal{M} (thus a set $\{\hat{\mathbf{y}}_{t,m}\}_{m \in \mathcal{M}}$) and given \mathbf{y}_{t+h} . $\mathbf{y}_{t,M}^*$ marks the theoretical absolute optimum of an ensemble M

We define a linear program minimizing the absolute loss of a combination ensemble below. We call its optimal solution, the Implicit Ensemble Loss, or E_{loss} ¹.

$$E_{loss}(\mathcal{M}, \mathbf{y}_{t+h}) =$$

Sets	\mathcal{M}	Models in ensemble
	T	Forecast horizon
Parameters	$b_{ij}, (i, t) \in \mathcal{M} \times T$	Matrix parameter representing model i forecast at t
	$y_t, t \in T$	Matrix parameter representing actuals
Variables	$x_i, i \in \mathcal{M}$	The weight of each model
	$z_t^+, z_t^-, t \in T$	Variable for modeling absolute value distance
Minimize	$\sum_{t \in T} z_t^+ + z_t^-$	Minimize total distance from actual
Subject to:	$y_t - \sum_{i \in \mathcal{M}} x_i b_{it} \leq z_t^+, \forall t \in T$	The actual value is larger than the forecast
	$-y_t + \sum_{i \in \mathcal{M}} x_i b_{it} \leq z_t^-, \forall t \in T$	The actual value is smaller than the forecast
	$\sum_{i \in \mathcal{M}} x_i = 1$	Weighted sum equals 1
	$0 \leq x_i, \forall (i) \in \mathcal{M}$	Each weight non-negative

Given this linear program, we can dissect the possible absolute error loss in a theoretically optimal solution. One can then think of the total loss a fitted model is experiencing as the sum of wrong weighing and the Implicit Ensemble Loss:

¹We note that this model implicitly finds the best weights to minimize MASE loss, this is because MASE \propto MAE. We find the best absolute weights, then multiply this value by an appropriate constant to find the global minimum MASE.

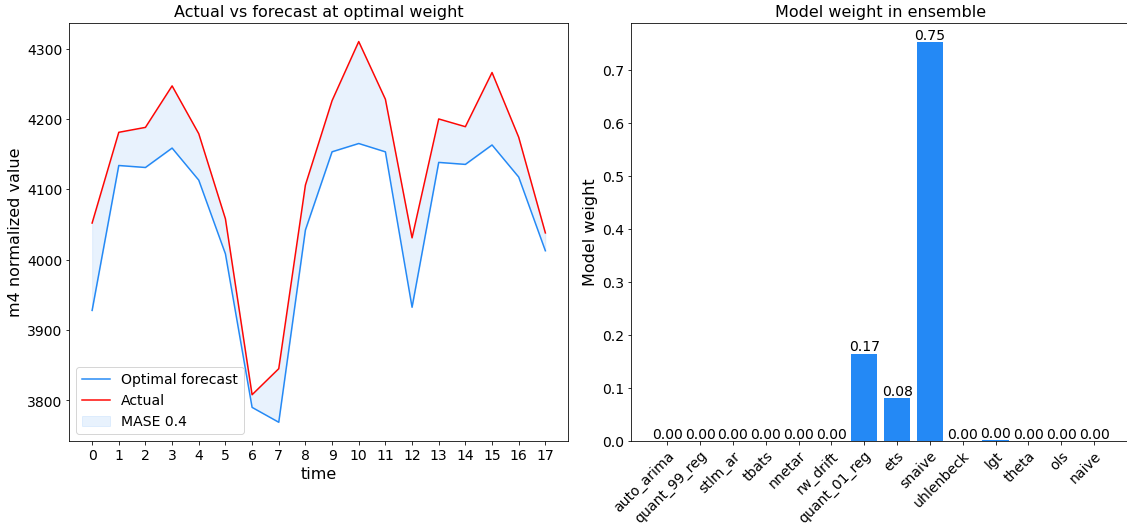


Figure 3: This is a plot where the optimal linear program solution clearly uses many forecasts and is successful. It is however not possible for the weight net to achieve a better result than 0.3 MASE given \mathcal{M}_{14} .

$$Total_{loss}(\mathbf{y}_t; \theta, \mathcal{M}) = P_{loss}(\mathbf{y}_t; \theta, \mathcal{M}) + E_{loss}(\mathcal{M}, \mathbf{y}_t, \mathbf{y}_{t+h}) \in \mathcal{L}_\Omega \quad (21)$$

To some extent, we should be able to reduce the loss P_{loss} from poor weighting through training, while E_{loss} is something given by choice of ensemble. This formula highlights that one should take care in choosing the ensemble composition. Indeed, even with an omniscient weighting entity, the designers of an ensemble algorithm can greatly reduce its upper bound accuracy even before training. To contextualize, our model below has $P_{loss} = NN(\theta) \in \hat{\mathbf{p}}_{\mathcal{M}}$, where $NN(\cdot)$ is an Artificial Neural Net. Although we do not know \mathbf{y}_{t+h} at time t , the model above gives a good method for making inferences on combination ensembles. Thus it is only used in $t_1 \geq t + h$ to gain knowledge of what caused a certain T_{loss} .

If we run the linear program over our M4 validation set, we find the best possible loss distribution below in Figure 5 and Figure 6 with our 14 models and the 9 models as in Montero-Manso et al., 2020 plotted respectively. Note that most of the new models from Section 2.5 are not given a large weight in the post facto forecast, but that they are non-negative, leading to meaning that FFORMA has a higher lower bound error. In the Implicit Ensemble Error for FFORMAs, naïve is given the least weight. Furthermore, in 0% cases, eight models are used in the optimal ensemble made by the linear program and almost no length six optimal ensembles. Although nowhere near using all 14 models, our approach still has a decreased lower bound loss than FFORMA since it uses a higher number of models.

We find the mean ex post facto MASE optimum for FFORMA to be 1.077 and 0.883 for our 14 models approach, on our held-out validation set, respectively.

3.4 Ensemble Building Heuristics

Selecting what models should be part of an ensemble is not a trivial task and will restrict the possibility of an optimal weight of predicting. We run a greedy search selecting a model for the ensemble by the model of all left, which results in the lowest MASE value. As such, we see how $E_{loss}(\mathcal{M})$ gradually diminishes with more models. We reason this is because of positive correlations between already selected models and possible candidates. For instance, notice that Naive and OLS are the last models added to the ensemble. This is possibly caused by the other algorithms already holding much of their predictive power. As such, adding them to the ensemble does not predict a series more accurately.

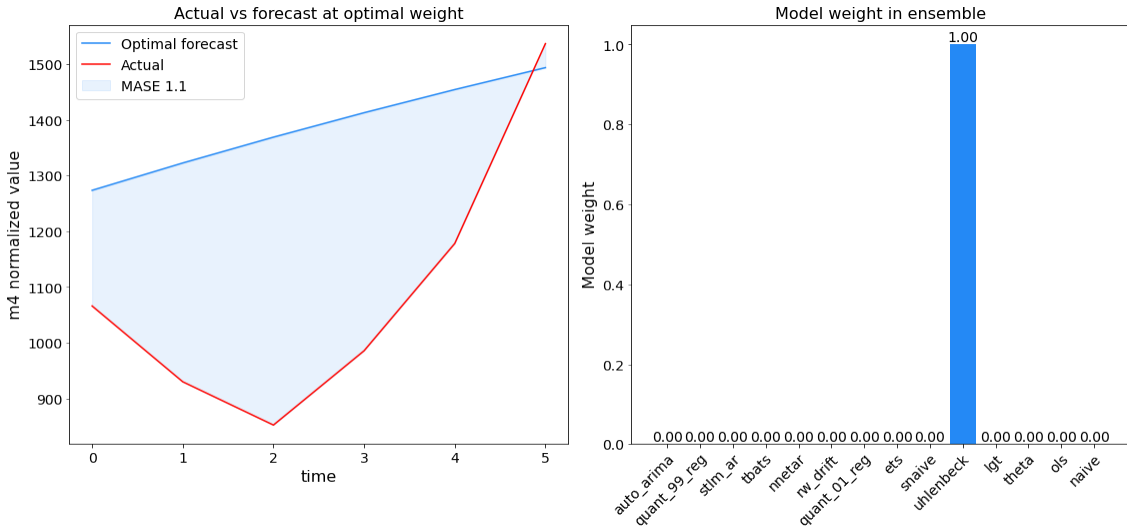


Figure 4: A optimal forecast where the linear program solution is no where near the actual times series. Furthermore, just a single forecast was used, implying that all other methods were even further from ground truth.

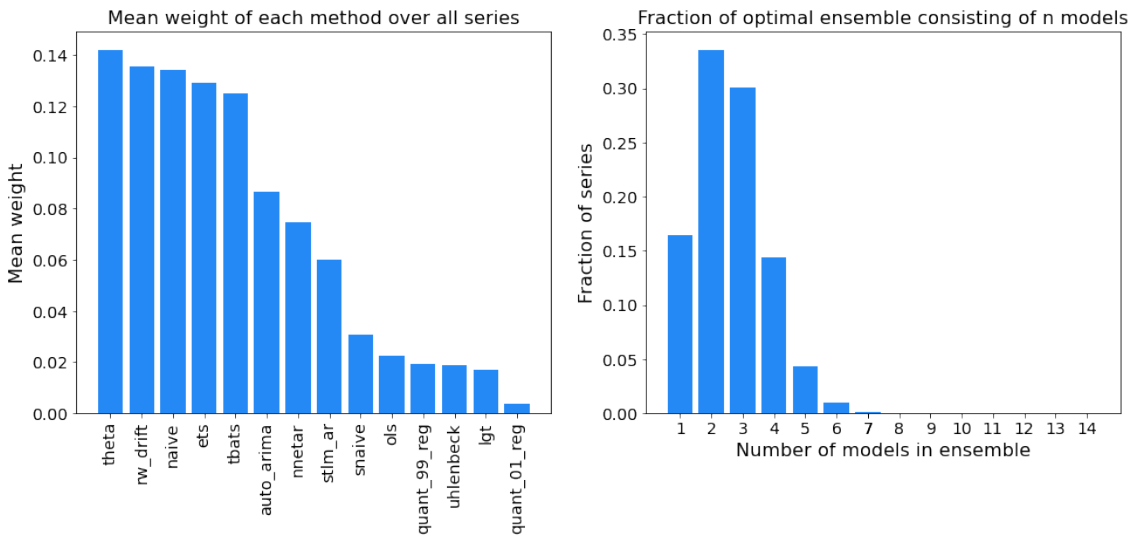


Figure 5: A display of the ex post facto best weight of the models in our 14 ensembles on our validation set. To the left is a display of mean weights for all models. Our newly implemented models are given a relatively low weight ex post facto. The right figure shows that 2-3 models ensemble is the most common combination. 4 models and more add up to around 20% of all ensembles.

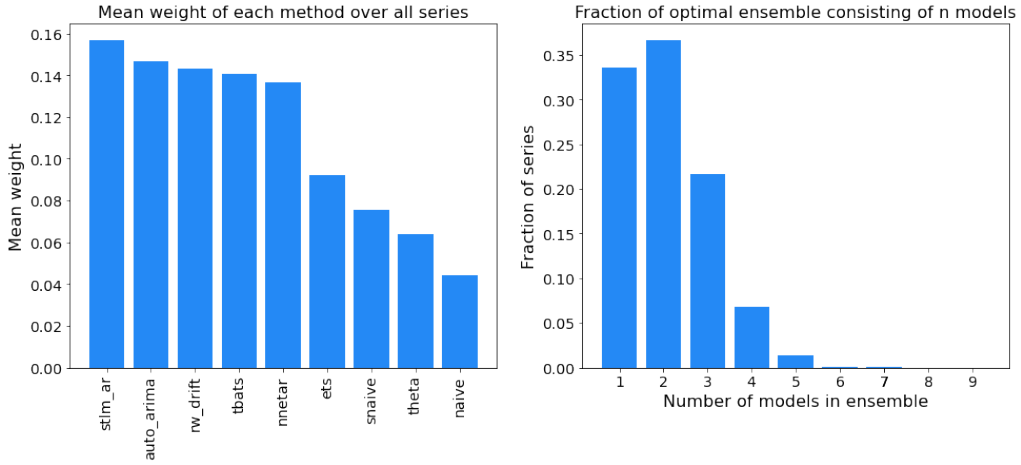


Figure 6: A display of the ex post facto best weight of the models of FFORMA on our validation set. To the left is a display of mean weights for all models. The right figure shows that 1-2 models ensemble is most common combination. 4 models our more adds up to around 7% of total optimal solution.

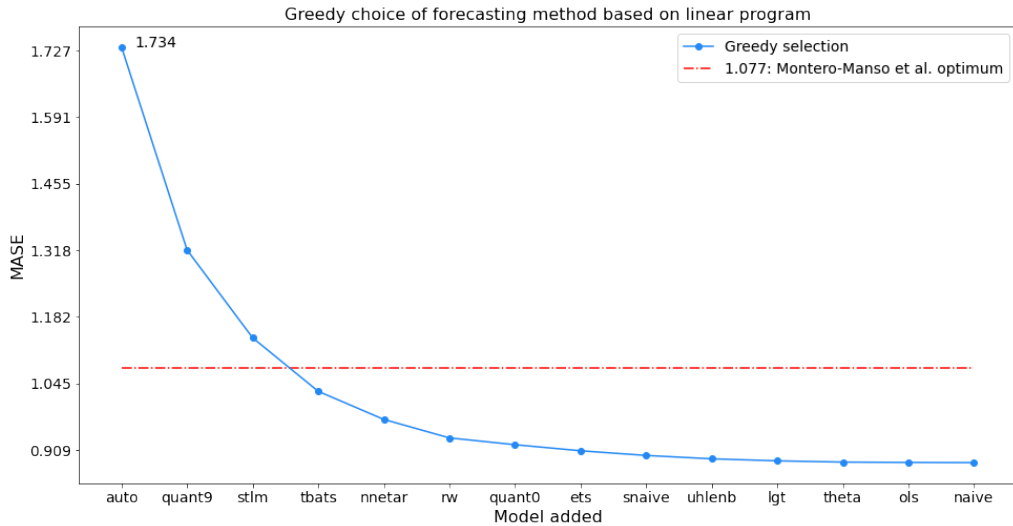


Figure 7: Greedy search for optimal ex post facto ensemble

Furthermore, one can note that the greedy result has an optimal ensemble error lower than that of FFORMA already at four models. Although this is ex post facto, it indicates how adding some models gives expression and that adding many statistical models gives a marginally decreasing loss reduction. One could then conclude that adding fewer models to make the weighting entities.

3.5 Model selection vs. model weighting theory

3.5.1 Optimal Loss of Model Combinations and Selections

One can prove that the ex-post-facto model selection approach has at least as high a loss as a model weighting technique.

Proof. Given a set $\mathcal{M} \mid |\mathcal{M}| > 1$ of models, $m \in \mathcal{M}$, $\mathcal{L} \in \mathcal{L}_\Omega$, and actual value \mathbf{y}_{t+h} . The ex post facto optimal combination loss will always be lower than model selection as $\hat{\mathbf{y}}_{t+h, \mathcal{M}}^* \subseteq \hat{\mathbf{y}}_{t+h, \mathcal{M}}^*$ since $\hat{\mathbf{y}}_{t+h, \mathcal{M}}^* = \hat{\mathbf{y}}_{t+h, \mathcal{M}}^* \iff \hat{\mathbf{y}}_{t+h, \mathcal{M}}^*|x_m = 1$. Thus, $\mathcal{L}(\mathbf{y}_{t+h}, \mathbf{y}_{t+h, \mathcal{M}}^*) \leq \min_{\forall m \in \mathcal{M}} (\mathcal{L}(\mathbf{y}_{t+h}, \mathbf{y}_{t+h, \mathcal{M}}^*))$.

Where $\min_{\forall m \in \mathcal{M}} (\mathcal{L}(\mathbf{y}_{t+h}, \mathbf{y}_{t+h, m}^*))$ is exactly the problem of ex post model selection.

And $\mathcal{L}(\mathbf{y}_{t+h}, \mathbf{y}_{t+h, \mathcal{M}}^*)$ is the problem of ex post model combination.

□

We find this interesting keeping the T_{error} formula in mind and the empirical findings of several studies. (Makridakis et al., 1982; Makridakis et al., 1993; Makridakis & Hibon, 2000; Makridakis et al., 2018) where ensembles seems to be outperforming single models, one explanation could be that the $E_{loss}(m) \geq E_{err}(\mathcal{M}) | m \in \mathcal{M}$

3.5.2 Computational proof of model weight ex-post superiority

We have already proved by computation that model selection ex post facto only amounts to 34% of optimal solutions with Montero-Manso et al. (2020)s ensemble, which reduces to 16% of optimal solutions when using our 14-ensemble. We can also calculate FFORMA's upper bound model selection score:

FFORMA	Mean	Variance
MASE Model Combination	0.944	2.558
MASE Model selection	1.053	2.707

Table 3: Table of the ex post facto MASE score for optimal model selection and optimal model combination for the FFORMA ensemble of nine models.

For the FFORMA ensemble, we can find the MASE loss ex post facto, finding the optimal weights of the combination problem and the optimal selection problem. In line with the results in Section 3.5.1 we see a 10.4% reduction in MASE and a 5.5% reduction in optimal solution variance in a combination vs. selection approach ex post-fact. This implies that Montero-Manso et al. (2020) with their current ensemble would theoretically be able to reduce their MASE by 32.1% with selection, and 39% keeping their combination ensemble framework.

3.6 Recurrent Autoencoder

We use a form of Recurrent Neural Networks, called Long Short-Term Memory network (LSTM), in an Autoencoder (AE) constellation, to extract features from a time series (TS). These features will later be provided as inputs for our final ensemble weighting model. By using an LSTM, the aim is to create features of a TS which are not obvious to humans, or even more so, features humans cannot themselves think of. Thus, combining human and NN feature extraction to leverage more predictive features of a TS in forecasting.

AEs are a tool for Non-Linear Principal Component Analysis (NLPCA) and can serve similar purposes like dimensionality reduction, visualization, and exploratory data analysis (Kramer, 1991). The main advantage of using an AE is that Principal Component Analysis (PCA) can find only linear relationships between variables, while the AE places no such restrictions on the variable interactions. Kramer (1991) proves that NLPCA can efficiently reduce dimensionality and produce a lower-dimensional representation that accurately resembles the actual distribution of the underlying system parameters.

A Deep Neural Net (DNN) architecture of LSTM cells was chosen to implement a time series feature extractor. The superiority of LSTMs for modeling complex temporal relationships is argued in Section 2.3. An Autoencoder (AE) is a DNN architecture used for unsupervised learning, which is ideal for this application as the goal is to generate features without human judgment or labeling. This is achieved by providing raw data as inputs to the model and scoring the model on how well it is able to recreate the input. This procedure becomes interesting once a bottleneck is added (the green box in Figure 8), which makes sure that the maximal number of parameters the model

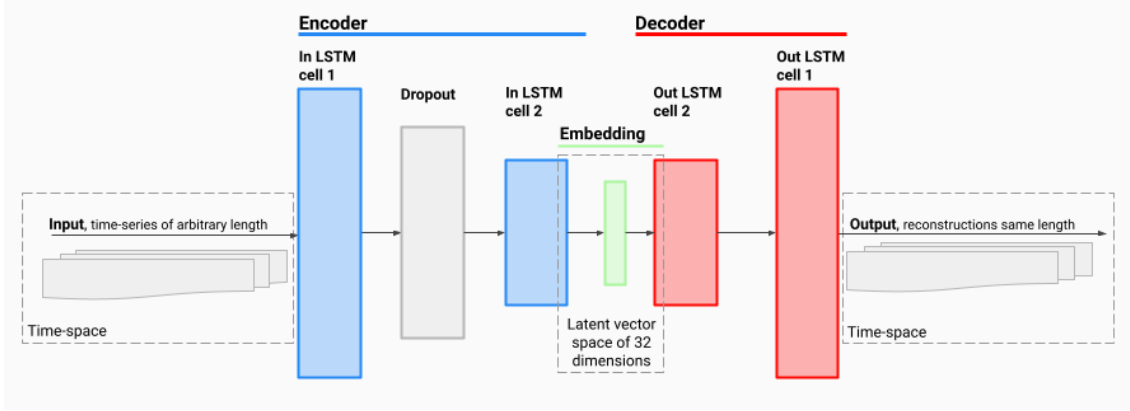


Figure 8: The LSTM model architecture. There are two LSTM layers on each side of a bottleneck. There is also a dropout layer between the two LSTMs in the encoder.

can work with is limited to be strictly less than the number of input features to be recreated. This forces the Autoencoder to learn how to represent the input in a lower-dimensional space, often called *latent vector space* or *vector embedding space*. Our concrete model takes TS of varying lengths and compresses them into a time-invariant vector of length 32 that exists in a vector space in \mathbb{R}^{32} .

Our architecture comprises two layers of LSTM cells on each side of the bottleneck or embedding. See Figure 8 for context. The part to the left of the blue embedding is called the Encoder, and the part to the right is the Decoder. During training, the whole system is trained to be able to replicate the input signal in the time-dimension from a compressed representation in \mathbb{R}^{32} . To successfully do this, the network has to learn how to extract the important features in a time series. During the inference phase, the Decoder is removed, and only the Encoder is used. This will thus produce vectors of a fixed size that represent time series of varying lengths for use in the model weighting network.

The hyperparameters used for training are summarized in Table 4. The hyper-parameters are decided on by thorough sweeps based on Bayesian search and Hyperband pruning of runs, as described in Li et al. (2017). The searches are conducted using the online service wandb.ai. In short, we found that normalizing data was essential due to the problem of exploding gradients. Both min-max scaling and standardization were tested, and standardization seemed to work the best. Furthermore, enough regularization, in the form of dropout and weight decay, was also essential to prevent overfitting (see Goodfellow et al. (2016) for an in-depth overview of regularization methods).

Parameter	Value
Epochs	500
Batch size	512
Embedding dim	32
Hidden dim	128
Learning rate	0.002
Optimizer	AdamW
Data-processing	Standardization
Dropout	20%
Weight decay	0.005
Max length	500

Table 4: Hyper-parameters used to train the final LSTM autoencoder model. These hyperparameters were decided through a qualitative guessing of appropriate ranges and several days of compute devoted to a Bayesian search over the space of hyperparameters with respect to validation loss.

During training, the loss quickly fell from the initial levels to around one-fourth within the first 100 epochs. During the remaining 300, the loss was only reduced marginally. However, both training

and validation loss fell in lock-step, signifying that we have not reached a state of over-overfitting.

3.7 LSTM Autoencoder Interpretation

3.7.1 Reconstruction Results and Interpretation

To validate that the network did indeed learn something, we constructed several different synthetic datasets, one of which can be seen in Figure 9. The dashed blue and red line is two different sine waves with random noise added. After training on the M4 data, the Autoencoder’s reconstruction is the blue and red lines. It has never seen these lines before. Still, it filters out the noise to a very high degree and captures the essence of the series. Synthetic data was used for this because it allows one to decide what percentage of the data is signal and noise. Furthermore, in this case, the embedding dim is of length 4, while there are 100 timesteps. As such, this Autoencoder embedding dimension must contain an abstraction of sine, which the Decoder can construct at least 25 times its input size.

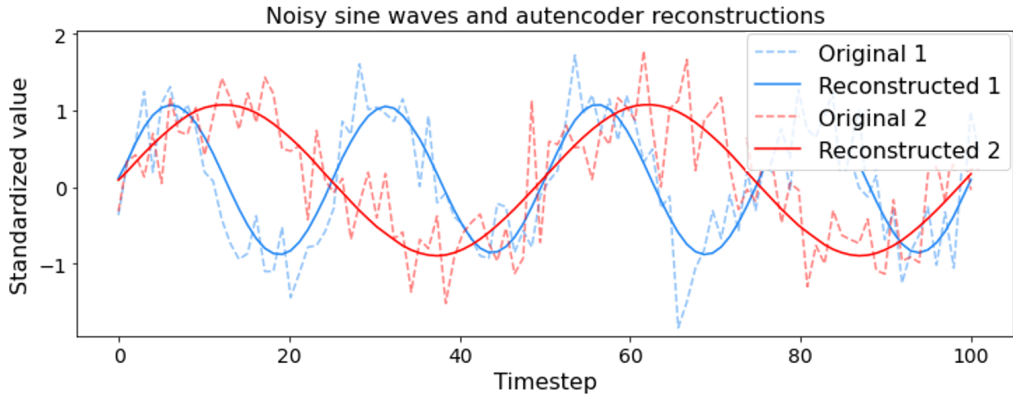


Figure 9: Two different noisy sine-waves and their reconstructions. The noise is clearly filtered out and only the smooth sine-waves remain. The embedding dim used to represent recreate the sine curve is of length 4, while there are 100 time steps, ergo the recreation must be based on a compressed abstraction of sine

In Figure 10 some examples of our actual AN is depicted. The reconstructions are done on the validation part of the M4 dataset, meaning that these are graphs the AN has never seen. Here, the Autoencoder is trained to reconstruct the last 1 000 data-points of longer series, or the full length for shorter series (in the example, all happen to be of length 400 or shorter). Once again, the network is, to a high degree, able to capture the essence of the time series, despite never having seen these series before and is limited to representing the whole series in a vector of length 32 ($<< 1000$, i.e., the length of each time-series).

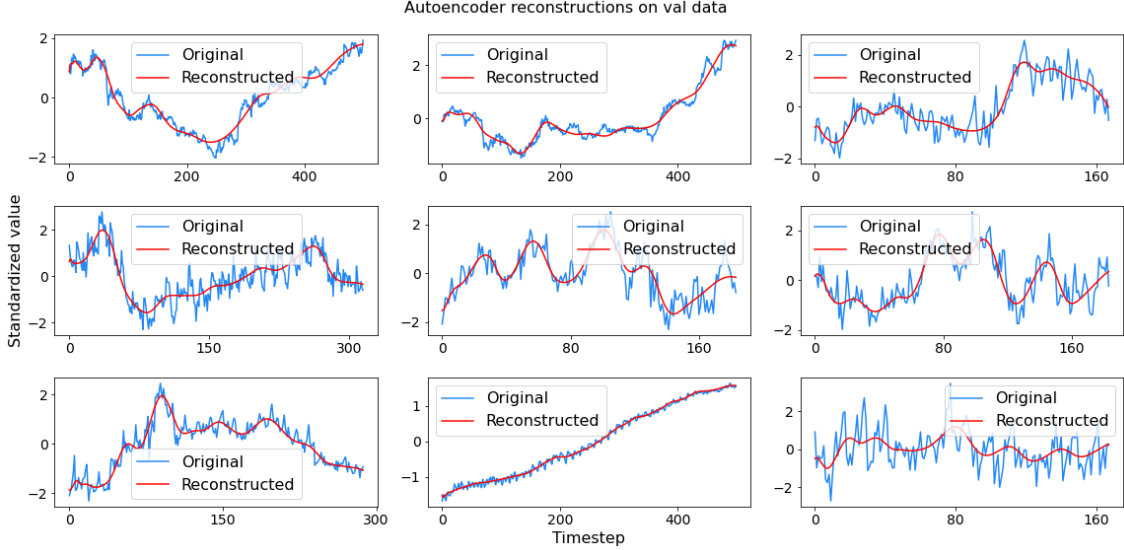


Figure 10: Original and reconstructed time-series from the M4 dataset of the validation partition, i.e. out-sample data. The autoencoder is able reconstruct many different types of time-series of different lengths, only based on a feature vector of length 32.

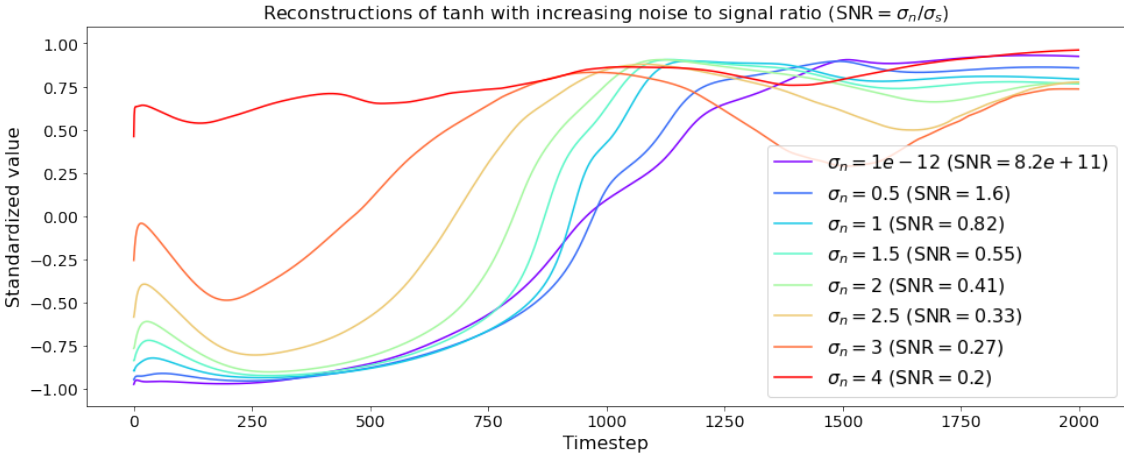


Figure 11: This figure depicts how the Autoencoder reacts to increasing noise. We generate a tanh function of 2000 data points. Then, iteratively, more and more random noise is added to it before it is given to the Autoencoder for reconstruction. The reconstruction is solid at minimal noise, shown with the purple line. The reconstruction has broken down at the other end of the spectrum, shown with the red line. This breakdown happens at around 2-3 σ for the noise generation process or a signal-to-noise ratio of ca. 0.35.

3.7.2 Measuring Importance of Features Generated by the Autoencoder

Neural Nets (NN) cannot be easily interpreted like, e.g., linear models. Therefore, more sophisticated ways of analyzing the relevance of variables are necessary. The technique of *feature permutation*, introduced by Breiman (2001), is a widely used technique. It works by iteratively breaking the relationship between the dependent variable and each feature one by one by randomly scrambling that feature across the dataset while keeping everything else in place. Then, the importance of a feature is defined as the increase in the loss from the baseline when that feature is scrambled (Breiman, 2001). We utilize this technique to analyze the interaction between our weighting model and the autoencoder feature in Section 4.3. Here the permutation importance procedure is run multiple times and subjected to t -ratio tests to investigate whether changes are

statistically significant (Student, 1908).

3.8 Automated Hyperparameter Search

One drawback with Deep Neural Nets is the large number of hyperparameters that must be set just right to achieve good results.

In Figure 12, the different combinations of hyperparameters and their corresponding validation loss can be seen. The most striking result from this plot is the observation that the model seems to prefer one hidden dimension, as well as considerable degrees of regularization in the form of dropout. Other conclusions to draw from the analysis are that, in general, larger batch size and a lower learning rate boosts performance.

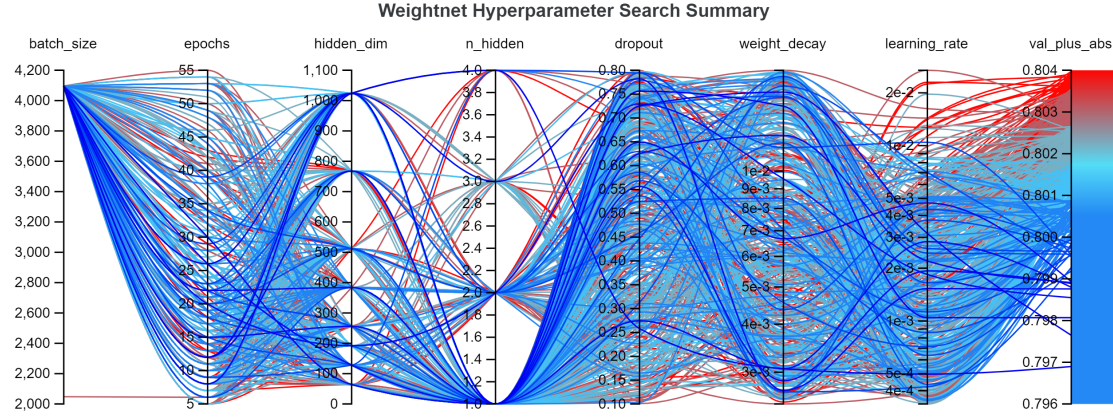


Figure 12: Summary over multiple runs with different hyperparameters and how they relate to final validation loss. Each line from left to right is one full training of the model with a unique set of hyperparameters characterized by where the line crosses the different lines for each hyperparameter. Deep blue lines achieved the best validation loss, and deep red is the worst.

3.9 Weight model

Our weight model as depicted by the step 3) box in Figure 2, is a Fully Connected Neural Network. It is trained on 80/20 training data, and converged quickly to what seems to be a local minimum. In Table 5 the hyperparameters of the model are found. Its inputs are statistical and LSTM generated features. The weight models outputs are 14 weights for each single statistical model in our ensemble.

Parameter	Value
Epochs	12
Batch size	4096
Hidden dim	1024
Learning rate	0.002
Optimizer	AdamW
Dropout	25.8%
Weight decay	0.003064

Table 5: The hyperparameters for our final weight model, the model is a fully connected neural network.

4 Results

The DONUT model presented above achieves a superior result to the FFORMA model by Montero-Manso et al. (2020), see Section 4.1 and Table 6. Furthermore, we find that our model’s predictions differ from the FFORMA model’s in several interesting ways, described in Section 4.2. Lastly, through analysis of feature importances, we find that our model heavily utilizes the automatically extracted features of the autoencoder to produce forecasts, described in detail in Section 4.3. Note: “DONUT” comprises the full approach and general model described, while “Fanciful” is the name of the specific trained model used to produce the results in the following.

4.1 M4 Test Data Forecasting Results

The final model achieves a result on the M4 test set of 0.830, 11.573, and 1.636 for OWA, sMAPE, and MASE, respectively. This result would give the “Fanciful” model the second place in the M4 competition by some margin, with an OWA of 0.008 better than Montero-Manso et al. (2020) and 0.009 off the first-place approach by Smyl (2020). In Table 6, one can see that the second to sixth place is separated by 0.010 in OWA score. Our model surpasses the second place by almost the same amount, signifying that the DONUT approach is a significant improvement.

Method	OWA	sMAPE	MASE	M4 rank
Smlyl	0.821	11.374	1.536	1
<i>DONUT Fanciful</i>	0.830	11.573	1.544	2 [†]
Montero-Manso	0.838	11.720	1.551	2
Pawlakowski et al.	0.841	11.845	1.547	3
Jaganathan & Prakash	0.842	11.695	1.571	4
Fiorucci & Louzada	0.843	11.836	1.554	5
Petropoulos & Svetunkov	0.848	11.887	1.565	6
Best single model (Theta)	0.897	12.309	1.696	18
Simple average	1.040	13.454	2.082	39

Table 6: Summary of our results compared to other relevant methods on the M4 dataset. Our method achieves a significantly better OWA result than the M4 second place, and a MASE better than both the first place and second place. [†]DONUT model did not enter competition but the rank is included to contextualize the result.

In Table 7 our result is broken down into the different categories and time intervals between successive observations of the M4 data set (termed the type or category, and period, respectively). The table shows that the model has differing forecasting ability for different types of series. Most remarkably, the model achieves a statistical significant OWA of 0.384 on Monthly Demographic data at a $\alpha = 0.001$ significance level. Furthermore, the Demographic type is overall the best at an OWA of 0.528. The only under-performing period in demographic is the daily, but this did not prove significant and comprises only 10 series, resulting in high variance and low impact. Furthermore, observe that the model also performs better than average for Macro data at 0.811, also statistically significant. This strengthens our hypothesis that some types of time series are easier to predict than others. Large, structural changes, like population growth or GDP growth are usually more stable than e.g. stock prices, and should therefore be easier to forecast.

Looking at the time intervals, one can observe that the model performs better than its average for Hourly, Monthly, and Quarterly data, and worse than average for Yearly, Daily, and Weekly data. In the case of the Hourly data, it seems there is a very specific type of series in the Other Category that the model responds well to. For Monthly and Quarterly it is presumably because there is the right combination of enough data and enough time between observation for them to be less noisy than e.g. daily. With that in mind, it is surprising to see the Yearly frequency performing much below par, breaking our hypothesis of sampling-frequency, i.e. easier prediction given longer time steps. The observation, however, could be a result of the Yearly periods populous Financial and Micro time series, both of which we might cause the model to under-perform.

	Demographic	Finance	Industry	Macro	Micro	Other	Mean
Daily	2.903	1.017***	1.142***	0.992*	0.801	1.040***	0.961
Hourly	NaN	NaN	NaN	NaN	NaN	0.682 ***	0.682
Monthly	0.384***	0.738***	0.721***	0.715***	0.752***	0.647***	0.689
Quarterly	0.671***	0.698***	0.622***	0.638***	0.659****	0.483***	0.650
Weekly	1.398**	0.786	0.863	1.204***	0.830	1.454	0.912
Yearly	0.996***	1.356***	1.420***	1.307***	1.205****	1.190***	1.289
Mean	0.528	0.912	0.844	0.811	0.854	0.881	0.830

Table 7: OWA loss for the method on the test set and for each subset of the data. Main finding is a OWA loss of 0.830, significantly better than Montero-Manso et al. (2020). Significance levels: * $\alpha = 0.05$, ** $\alpha = 0.01$, and *** $\alpha = 0.001$.

Interestingly, Financial series, in general, the model predicts with lower accuracy which would strengthen our hypothesis of type. For Monthly and Quarterly Financial data, however, it does not seem particularly hard to predict. This is a surprising finding and non-trivial to analyze the reason for since it is not known what process produced the different time series (as the M4 data is anonymized).

In Figure 13, Figure 14, and Figure 15, the ways the DONUT model, and The Fanciful incarnation in particular, weights the 14 models in the set of available models, is depicted. Figure 13 displays an example of a good forecast with a MASE of 0.5 and the associated weights produced by a combination of ARIMA, TBATS, and Random Walk. Figure 14 shows an example of a bad forecast with MASE loss of 4.4, with associated weights assigned to each model in the ensemble for the forecast. Here, the model used 0.8 of Seasonal Naïve, and 0.13 of Exponential Smoothing, which did not yield a good result. It also looks like the series had a structural break that made it hard to forecast for the component methods.

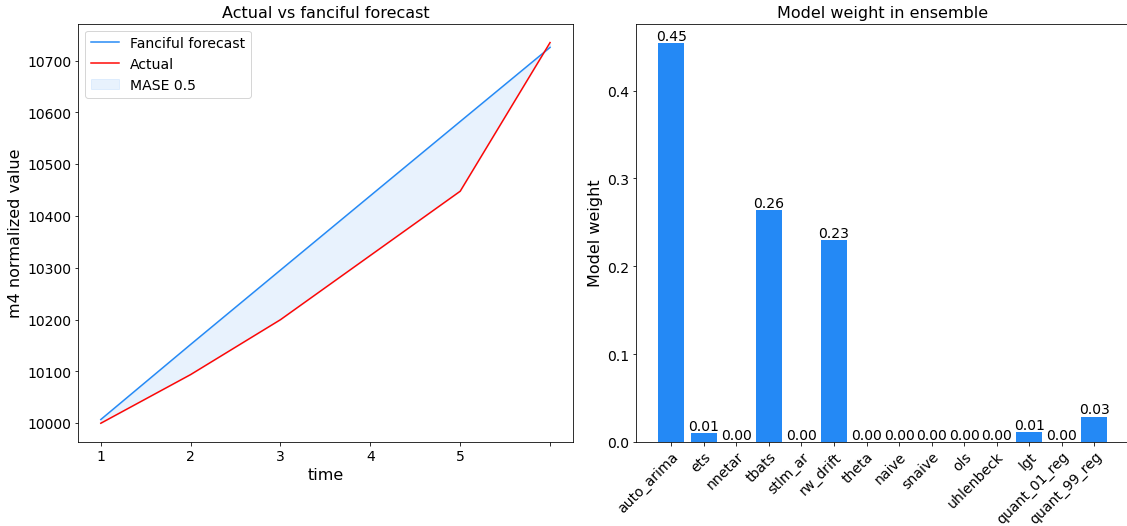


Figure 13: Left, the actual value compared to the forecast for a successful forecast. Right, the weights assigned to each model in the forecast on the left.

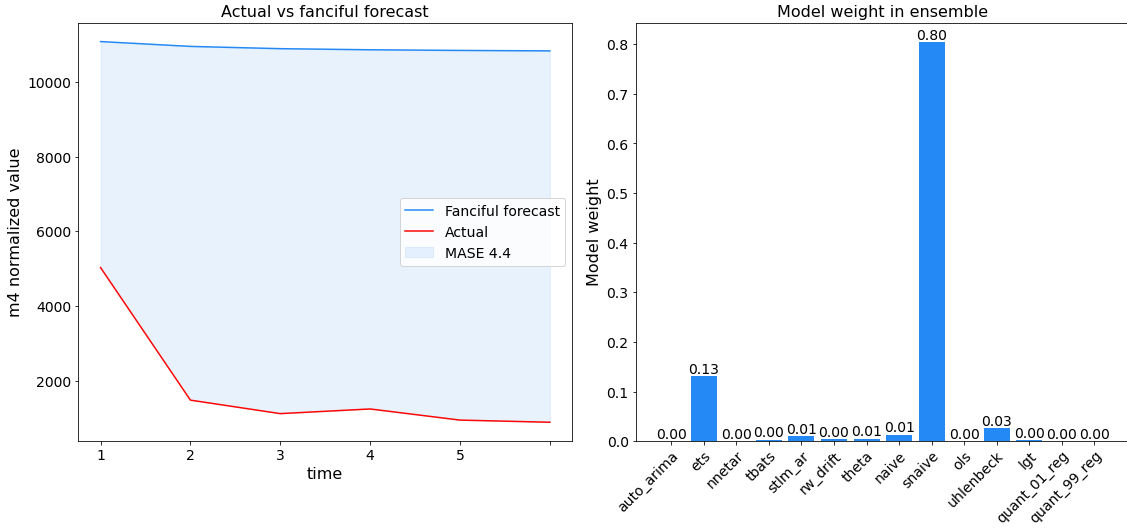


Figure 14: Left, the actual value compared to the forecast for a successful forecast. Right, the weights assigned to each model in the forecast on the left.

In Figure 15 it is interesting to see that the most popular methods were TBATS with the highest mean weight out of any model, with ARIMA, LGT, and Exponential Smoothing relatively equal to each other at a slightly lower mean weight. OLS and Quantile regression with $\tau = 0.01$ was virtually not used, which is somewhat surprising given our rationale for adding them. We reason this might be because the Random Walk With drift model of FFORMA, is highly correlated with the model. Ornstein-Uhlenbeck is more popular than naive. Furthermore, it is very evident that DONUT Fanciful uses combinations of many different forecasting techniques at a high rate, as seen on the right in Figure 15, and remarkably ensembles consisting of 6-10 models seem most common. This is also another piece of evidence in favor of combinations over selection.

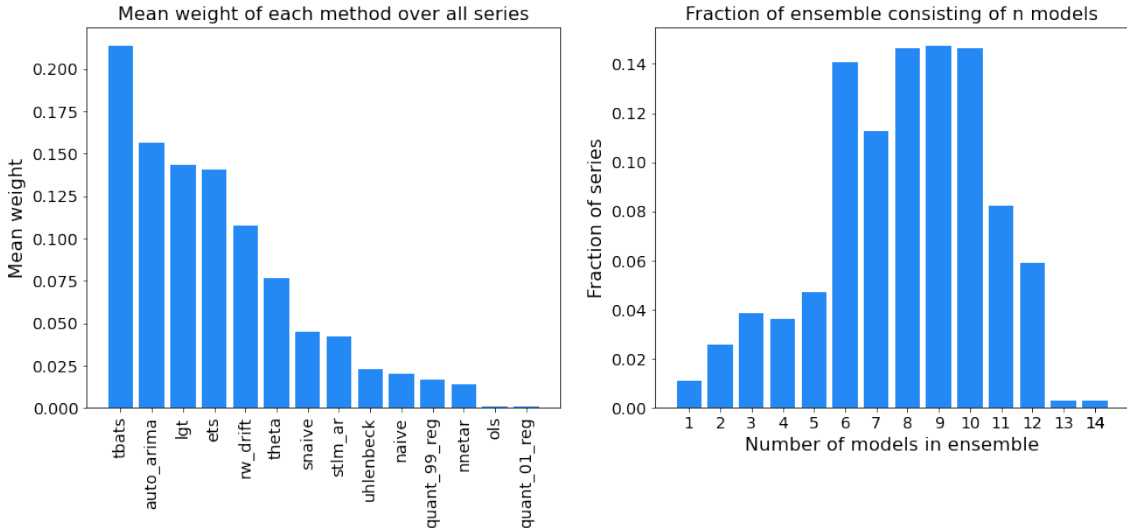


Figure 15: Left, a bar chart summarizing the mean weight each separate forecasting model was assigned by DONUT Fanciful over the entire test set. Right, the percentage of series for which DONUT Fanciful uses ensembles of a given size.

4.2 Performance Comparison to FFORMA model

Since the DONUT approach is based mainly upon the FFORMA model by Montero-Manso et al. (2020) with a goal of improving the approach by making fewer assumptions, that our performance

is improved significantly. In Table 8, a simple comparison is made. The DONUT Fanciful model improved the main metric of OWA by 0.008, which yields statistically significant difference with an associated p -value of 0.6%. This is an uplifting finding, and we find that this is some evidence in favor of reducing the assumptions a model rests on.

Δ OWA	t-statistic	p-value
-0.008	-2.510	0.006***

Table 8: OWA improvement from FFORMA, with t-statistic and one sided p-value with $H_0 =$ FFORMA mean

It is worth mentioning that a 0.008 OWA improvement would lead the sixth place competitor to take the second place in the m4 competition. As such, the improvement is noteworthy in the context of which it occurs. Even more so, one can look at what categories of series our net is differing from FFORMA. In Figure 16 it is evident that our model performs better on Financial Daily series, by a margin of .07. We are beat in combinations such as Micro, Weekly and Demographic Weekly. But two sets of categories contain 112 and 24 series, respectively as seen in Table 1 .

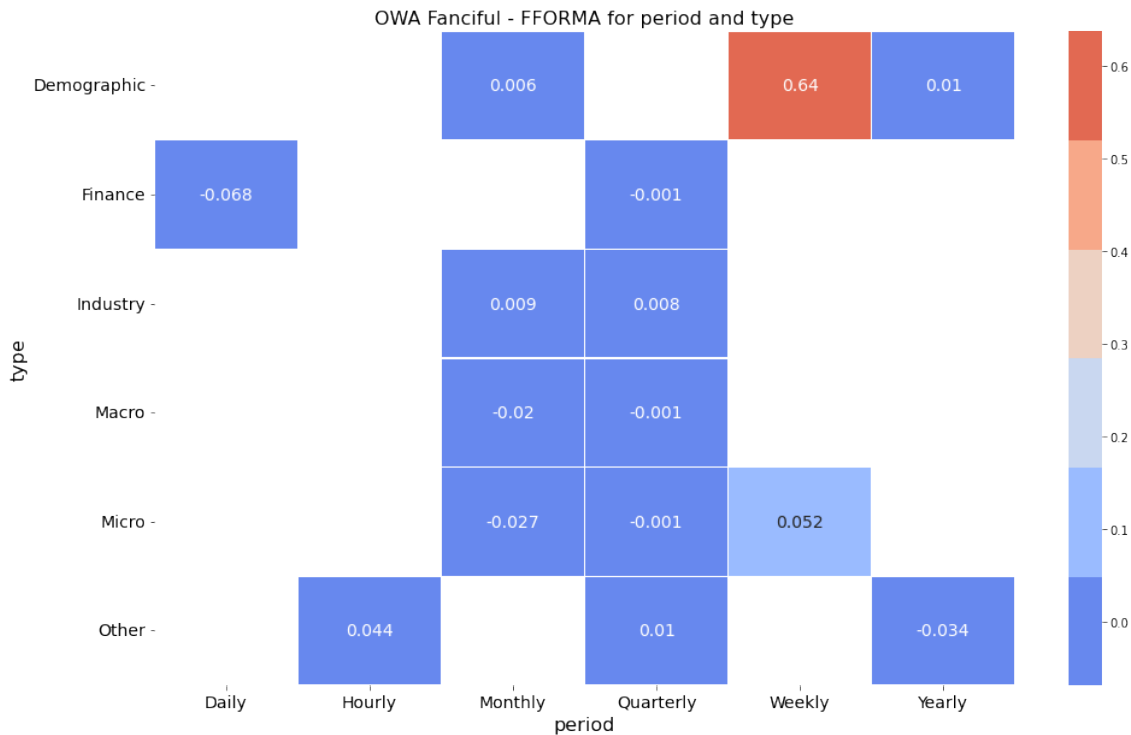


Figure 16: Colored boxes has p -value < 0.05 , $\mu_0 = \text{mean}(\text{row}_{\text{box}})$: Our fanciful model has a mean OWA of 0.068 less than FFORMA for daily financial series, $n=1,559$. FFORMA relatively strongest in the demographic, weekly category but this has $n=24$.

4.3 Feature-Importance Results

To discern whether the automatically extracted features of the autoencoder had any predictive relevance, we calculated the permutation feature importance scores for all features and compared them. An overview of the importance of each feature for the model's forecasting accuracy is presented in Figure 17 and Table 9. The feature importances are calculated by scrambling each feature of the input, yielding that feature meaningless for predictions. Then, by running the same model over the partially scrambled data one can record the deviation of the resulting OWA loss compared to the baseline OWA loss for all series. A larger increase in loss (decreased accuracy) means that that feature was more important for the prediction. Thus, the length of each bar

signifies the predictive power of the corresponding variable for the model. See Section 3.7.2 and Breiman (2001) for more details.

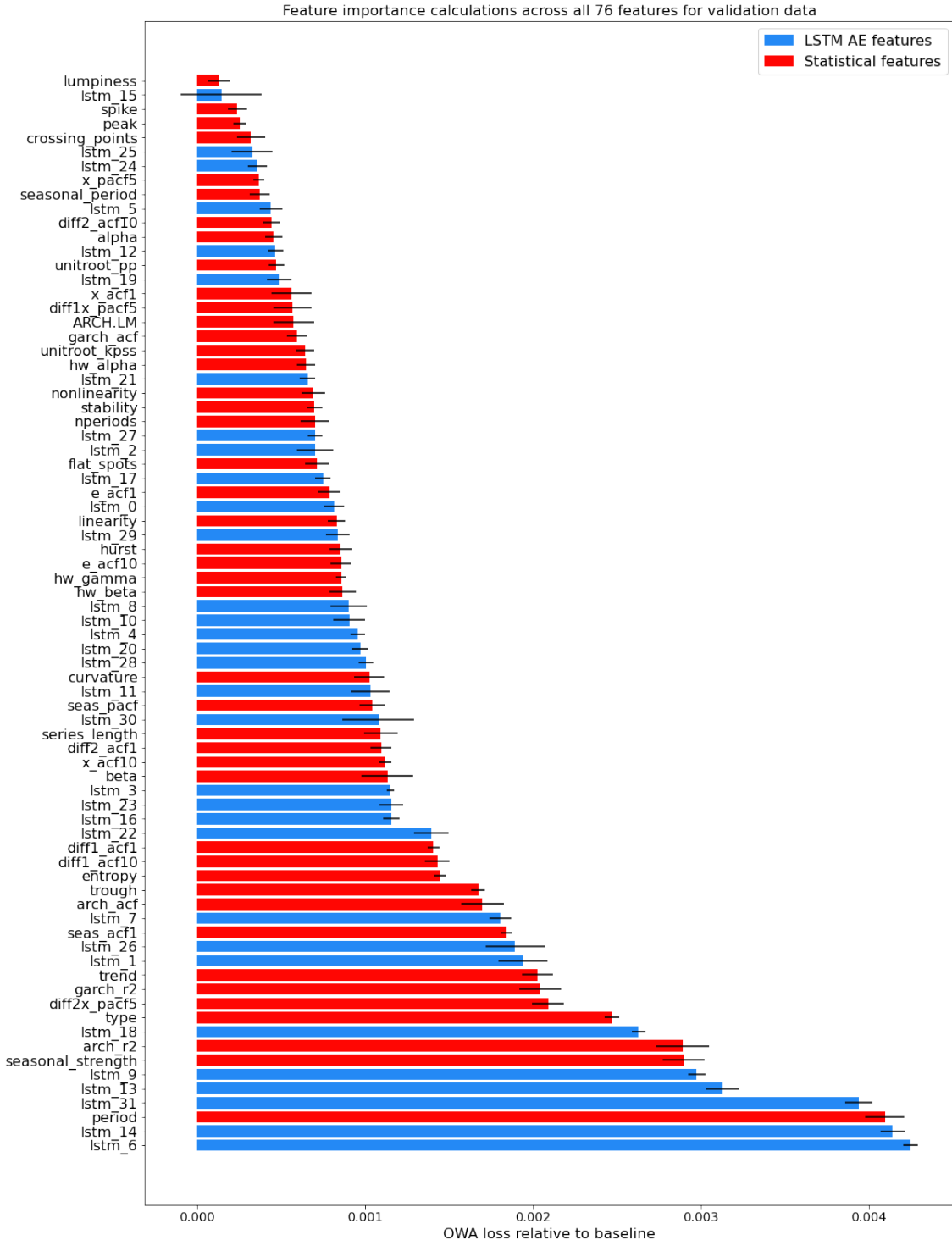


Figure 17: A visual representation of the feature importances for the 76 features our model uses. The features are listed in decreasing importance along the positive y-axis and x-values gives the deviation in OWA from the baseline when that feature is randomly permuted. The features generated by our Autoencoder are blue and the statistical features by Montero-Manso et al. (2020) are red. Several LSTM Autoencoder features have a high importance.

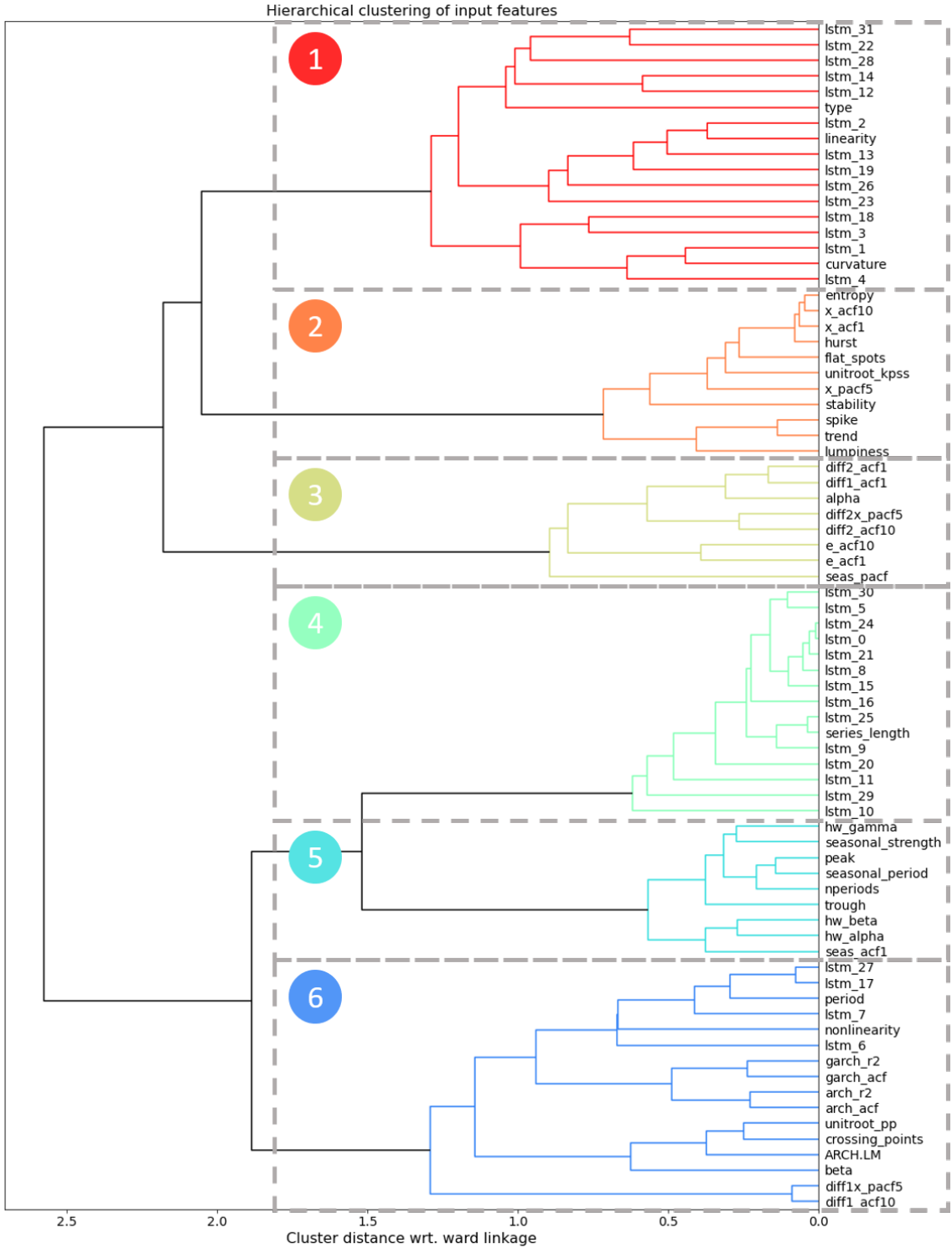


Figure 18: Hierarchical clustering of the correlation between all 76 features according to the ward's linkage. There are formed six distinct clusters of features. There is furthermore a tendency towards clustering among the statistical features and among the LSTM features.

Based on the clustering results in Figure 18, we also measured the permutation importance of all features within clusters, to see what feature clusters are most important, seen in the first plot in Figure 19. This is also compared to permutation importances for all statistical features used by Montero-Manso et al. (2020) together and all lstm features proposed here together (middle plot in Figure 19), as well as importance for all features used together (rightmost plot in Figure 19).

What we observe is that the first cluster is by far most important with an OWA increase of 0.06 when scrambled. This alone deteriorates the result significantly, as the resulting OWA places several places lower on the leader-board, but still slightly outperforms the Theta model alone. The remaining clusters have smaller importances but are still having a significant impact. Interestingly, the top two clusters, Cluster 1 and Cluster 4, consists mainly of LSTM features. Also, the least important clusters, Cluster 2, 3, and 5, contain no LSTM features.

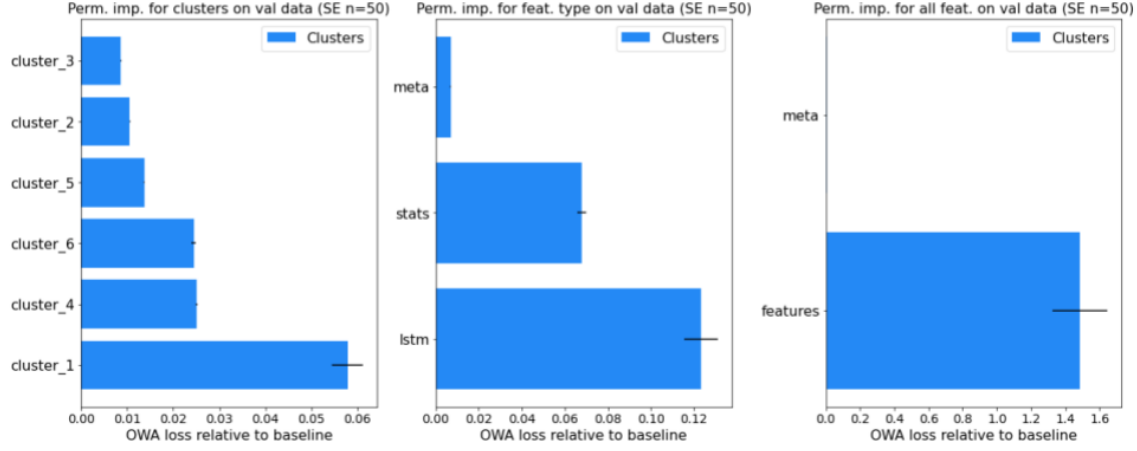


Figure 19: A plot showing the permutation importances (perm. imp.) when scrambling (1) all features in the different clusters defined in Figure 18, (2) both meta variables alone (type, period), all statistical features alone, and all lstm features alone, and (3) all features that are not the meta variables (type, period), from left to right, respectively.

In Table 9, we have randomized all features five times, and provide p -values for all feature importances, sorted according to decreasing importance. In the t -test, the null hypothesis, H_0 , is that the randomization of the column does not have an effect on our nets predictive power, i.e. that that feature has no predictive usefulness for the model’s ability to select appropriate combinations. Below when we use the term “Importance,” it refers to a relatively large increase in loss when scrambling the entire column of that feature, in the procedure described above.

It is evident that Period is the most important statistical feature for prediction for the Fanciful weighting model. Seasonal effects are also important for our weight net as seasonal_strength is the second most important statistical feature, a result which coincides with the findings of Makridakis et al. (1993). Furthermore, Arch_2 which is the R^2 of a AR model is also an important statistical feature. Furthermore, garch_r2 which is the R^2 value of an AR model applied to variance, or as we interpret it, the predictability (homoskedasticity) of the variance of a series, is the 5th most important category of the statistical features.

The LSTM features have a high importance, combined with an inability to reject the null hypothesis. 4 out of 5 the first 5 most important features are generated by the LSTM and 7 out of the top 10. Thus, like the encoder, our weight net is able to extract information from these novel time series features which is important for the weight it produces. lstm_6, lstm_14 are the first and second most important feature, even higher than that of period. This is surprising in the sense that some lstm values seem more important but we postulated that “type” and “period” was important for the network make apt predictions.

There is not a single null hypothesis features which we are able to reject at the 5% significance level. Still some features are both less significant and less important than others. Peak, Spike and Lumpiness, the strength of the peak, spikiness and lumpiness (as defined by Montero-Manso et al. (2020)) seems both least important and is among the least significant. There are also lstm such as lstm_15 and lstm_19 which are less important and less significant than other features.

Furthermore, it is interesting to note that even the most important features increase the loss by a mere 0.004 in OWA loss. That means that removing one of the top features alone would not make

the resulting OWA higher than what Montero-Manso et al. (2020) achieved. This can be viewed as a strength and makes sense in the context of how the network is trained. We have employed a high degree of dropout regularization into the training, meaning that the network is trained under circumstances of high noise—resulting in a model highly robust to perturbations.

Lastly, its worth mentioning that our weight net can be viewed as a function $P_{loss}(\theta_{lstm}, \theta_{stat})$ which we do not know the shape of and can in theory be an arbitrarily complex function. This means that Figure 17 does not say anything about relationships or interactions between these variables, but rather how each variable impact the model by themselves.

4.4 Comparison to FFORMA in input space

There is also a notion of series simply being easy to predict, which could cloud some of the results in this paper. Below we find that in input space, our LSTM features clearly demonstrates patterns of low OWA loss, and furthermore show superior to FFORMA, when certain conditions are met. We note that where there is white space in the figures of this subsection we either have no entries or a $p-value > 0.05$, where the null is that the population mean is that of the corresponding row for each box.

Firstly, seasonality and variance interpretations gives logical sense in the losses of our weight models predictions. Figure 20 shows that for our model, seasonal strength correlates with a low OWA, as indicated by a strong blue color. The Demographic series seems to be most easily predicted when seasonal strength increases. Furthermore Figure 21, shows behavior where loss on one the right hand side (where volatility is heteroskedastic) is higher than in the left hand side, where volatility is likely to be homoskedastic. That our perceived OWA loss is segmented in these rational ways when responding to seasonality and variance gives us reason to believe that our weighting entity performs rationally, weighting models which account for seasonality when it is present, and performing poorer when variance becomes more chaotic.

Figure 22 shows that our weighting model show a behavior when the input value of `lstm_6` is changed. Although we do not know how to interpret the machine learned feature, we can deduce that with statistical significance an increase in `lstm_6` makes our weight model more accurate.

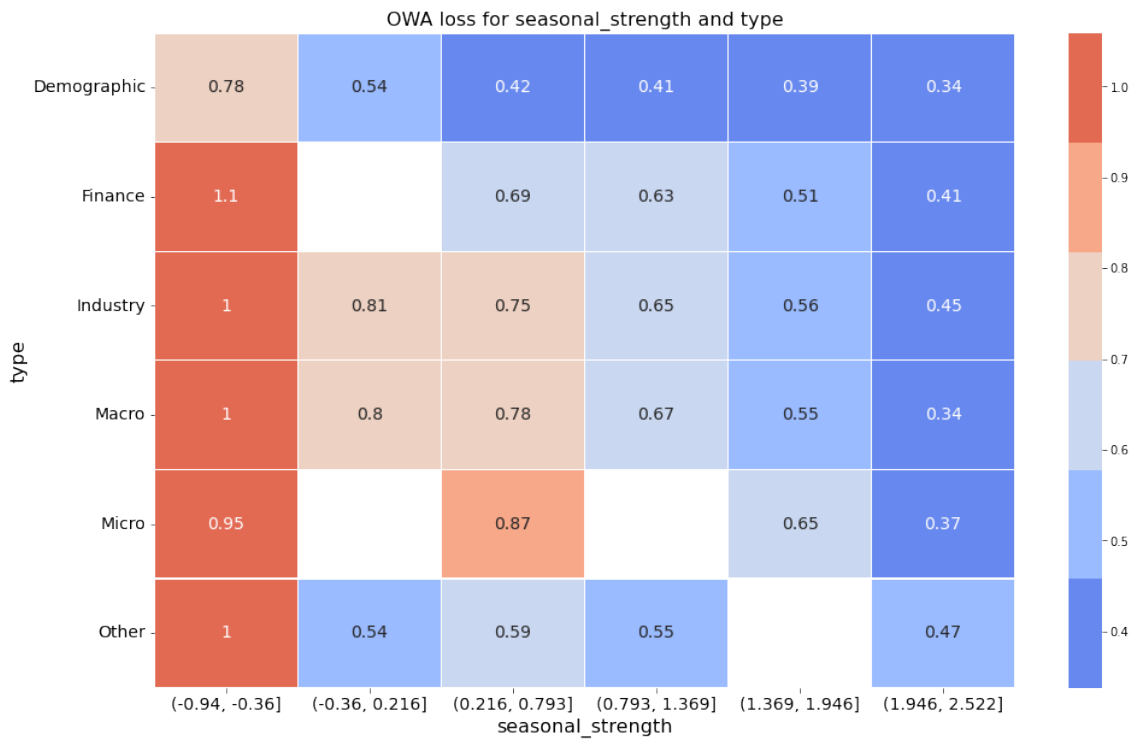


Figure 20: $p - value < 0.05$: A strong seasonal strength correlates with a low OWA, as indicated by a strong blue color. The Demographic series seems to be most easily predicted when seasonal strength increases.

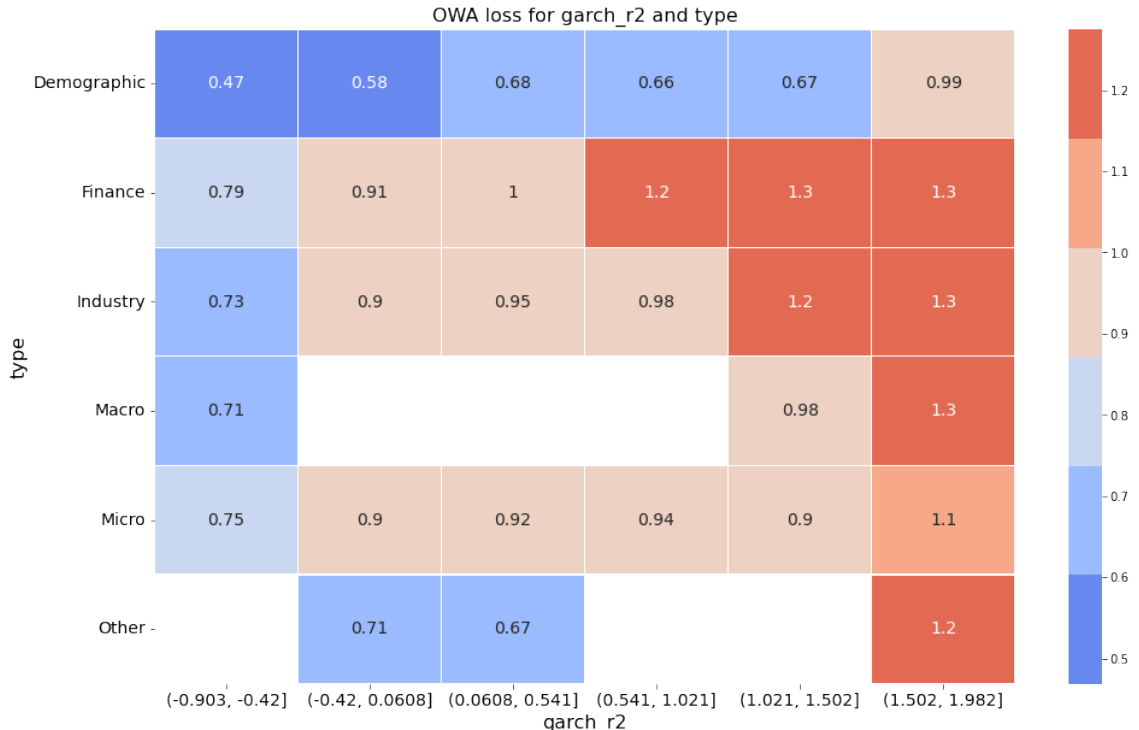


Figure 21: $p - value < 0.05$: Garch_r2, a measure of homoskedastic variance, also clearly correlates with a reasonable behavior from Fanciful sweep. Note how as the volatility measure increases, so does the difficulty of predicting, as indicated by a red color.

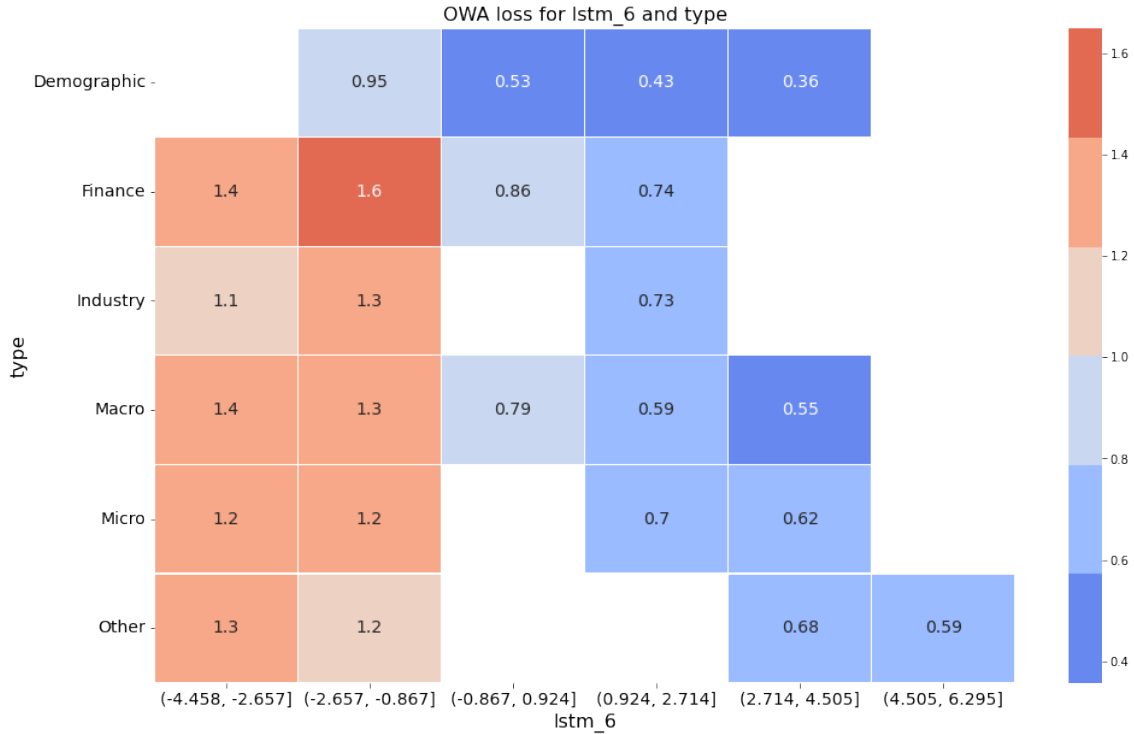


Figure 22: $p - \text{value} < 0.05$: Shows how `lstm_6` also correlates with predictability. As `lstm_6` increases all of the series seem easier to predict. The Autoencoder have provided information which correlates with a decrease in loss

It is interesting to view these results not in a void, but compared to FFORMA, to see if the LSTM features provide insight or relevant information where the statistical features do not. In Figure 23 the values in the cells are the mean of the OWA of DONUT Fanciful less OWA FFORMA and in the relevant split of feature values. As seasonality decreases, and the value of `lstm_31` increases our weight model is increasingly outperforming FFORMA as seen by the improving blue color to the left hand side. FFORMA does not have access to this the machine learned time series feature and it indicates that `lstm_31` holds information which can be useful when seasonality is not present. Lastly Figure 24 shows a relationship between two lstm features which looks to be non-linear, this coincide with the aforementioned findings of Kramer (1991) and non-linear properties.

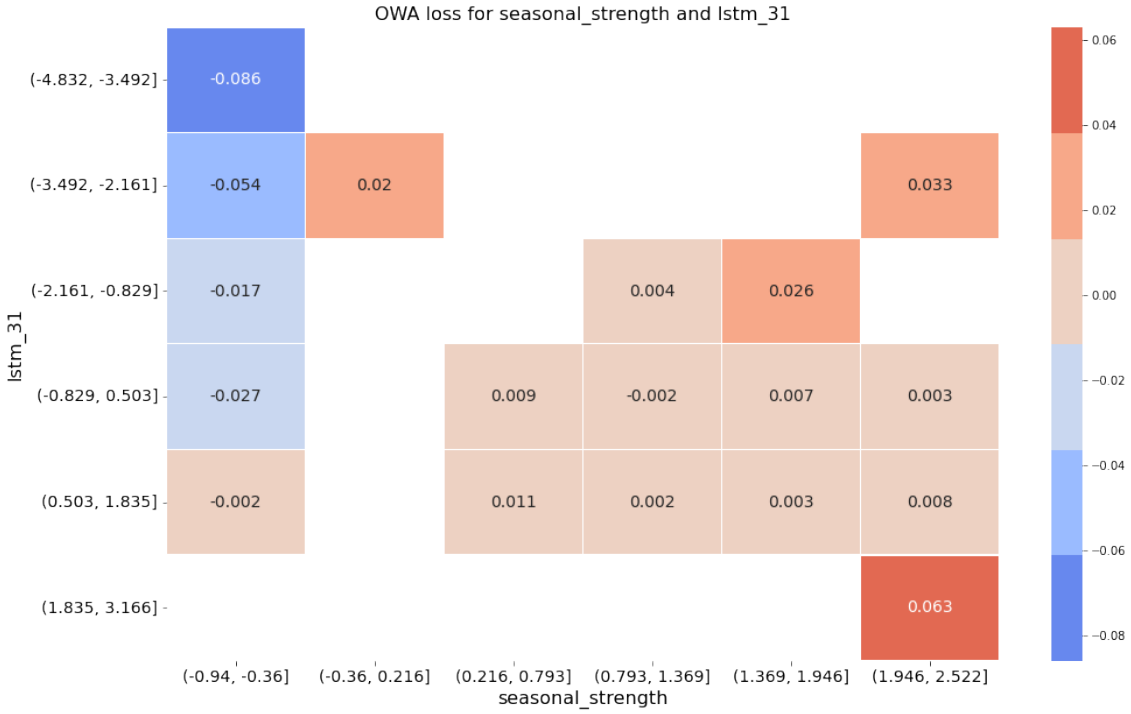


Figure 23: $p - value < 0.05$: When plotting lstm_31 against seasonal strength, again it seems like the auto generated feature offers extra predictive power to our net compared to FFOMA, as seasonality decreases. Note how the top right corner, has a OWA decrease of .86, with $p < 0.05$

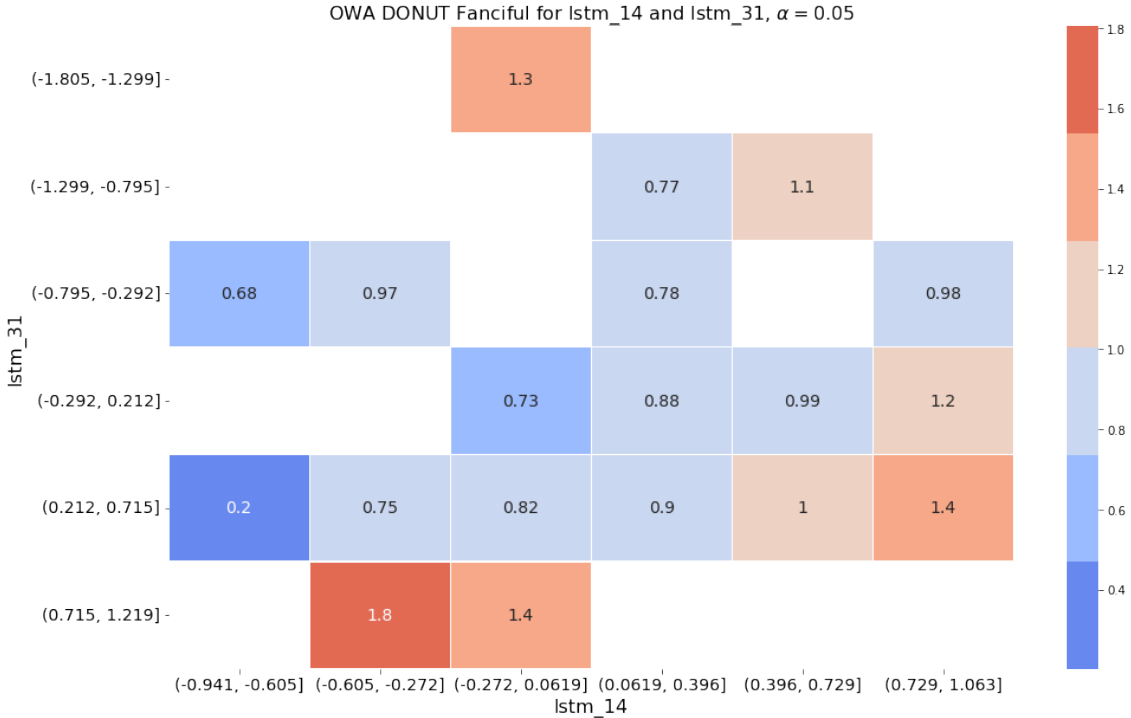


Figure 24: $p - value < 0.05$: When both lstm_31 and lstm_14 take on values near their medians, the DONUT mode does better than its average by a significant. This particular combination seem to elicit a non-linear relationship between the variables.

	lstm_6	lstm_14	period	lstm_31	lstm_13	lstm_9	seas_str	arch_r2	lstm_18	type
Importance	4.2e-03	4.1e-03	4.1e-03	3.9e-03	3.1e-03	3.0e-03	2.9e-03	2.0e-03	2.6e-03	2.5e-03
t-stat	2.6e+01	3.3e+01	3.0e+01	1.5e+01	1.3e+01	2.6e+01	2.2e+01	4.2e+01	2.5e+01	1.9e+01
p-value	(1.2e-05***)	(5.3e-06***)	(7.5e-06***)	(1.3e-04***)	(1.9e-04***)	(1.3e-05***)	(2.7e-05***)	(1.9e-06***)	(1.5e-05***)	(4.8e-05***)
Importance	2.1e-03	2.0e-03	2.0e-03	1.9e-03	1.9e-03	1.8e-03	1.8e-03	1.7e-03	1.7e-03	1.4e-03
t-stat	2.7e+01	1.8e+01	2.5e+01	2.4e+01	2.3e+01	1.3e+01	9.2e+00	9.9e+00	2.8e+01	1.8e+01
p-value	(1.1e-05***)	(5.5e-05***)	(1.5e-05***)	(1.7e-05***)	(2.0e-05***)	(2.2e-04***)	(7.8e-04***)	(5.9e-04***)	(1.0e-05***)	(6.1e-05***)
Importance	1.4e-03	1.4e-03	1.4e-03	1.2e-03	1.2e-03	1.2e-03	1.1e-03	1.1e-03	1.1e-03	1.1e-03
t-stat	1.0e+01	1.3e+01	2.6e+01	2.2e+01	9.5e+00	1.1e+01	1.1e+01	2.3e+01	1.1e+01	1.5e+01
p-value	(5.0e-04***)	(1.8e-04***)	(1.3e-05***)	(2.4e-05***)	(6.8e-04***)	(4.5e-04***)	(3.5e-04***)	(2.2e-05***)	(4.5e-04***)	(1.1e-04***)
Importance	1.1e-03	1.0e-03	1.0e-03	1.0e-03	1.0e-03	9.7e-04	9.6e-04	9.1e-04	9.0e-04	8.7e-04
t-stat	7.9e+00	1.4e+01	1.3e+01	1.6e+01	1.3e+01	1.2e+01	1.7e+01	1.6e+01	1.2e+01	2.5e+01
p-value	(1.4e-03**)	(1.7e-04***)	(2.0e-04***)	(9.6e-05***)	(2.0e-04***)	(2.4e-04***)	(7.8e-05***)	(8.0e-05***)	(2.4e-04***)	(1.5e-05***)
Importance	8.6e-04	8.6e-04	8.6e-04	8.4e-04	8.3e-04	8.2e-04	7.9e-04	7.5e-04	7.1e-04	7.0e-04
t-stat	9.1e+00	6.8e+00	9.5e+00	1.3e+01	1.4e+01	1.7e+01	5.7e+00	1.5e+01	1.8e+01	7.8e+00
p-value	(8.0e-04**)	(2.4e-03**)	(6.8e-04**)	(1.8e-04**)	(1.8e-04**)	(7.2e-04**)	(4.6e-03**)	(1.0e-04**)	(5.1e-05**)	(1.4e-03**)
Importance	7.0e-04	7.0e-04	7.0e-04	6.9e-04	6.6e-04	6.5e-04	6.4e-04	5.9e-04	5.8e-04	5.7e-04
t-stat	1.3e+01	7.6e+00	1.3e+01	1.0e+01	9.9e+00	9.5e+00	1.5e+01	1.5e+01	1.3e+01	9.8e+00
p-value	(1.8e-04**)	(1.6e-03**)	(2.3e-04**)	(5.4e-04**)	(5.9e-04**)	(6.8e-04**)	(1.2e-04**)	(1.2e-04**)	(2.2e-04**)	(6.1e-04**)
Importance	5.6e-04	4.9e-04	4.7e-04	4.7e-04	4.6e-04	4.5e-04	4.4e-04	3.7e-04	3.7e-04	3.6e-04
t-stat	3.2e+00	4.0e+00	7.8e+00	2.0e+01	5.4e+00	1.2e+01	9.5e+00	7.3e+00	4.8e+00	7.2e+00
p-value	(3.2e-02*)	(1.6e-02*)	(1.5e-03**)	(3.4e-05**)	(5.5e-03**)	(3.0e-04**)	(7.0e-04**)	(1.9e-03**)	(8.7e-03**)	(2.0e-03**)
Importance	3.3e-04	3.2e-04	2.5e-04	2.4e-04	1.5e-04	1.3e-04	1.3e-04	1.3e-04	1.3e-04	1.3e-04
t-stat	6.8e+00	8.1e+00	4.9e+00	4.0e+00	2.9e+00	4.0e+00	2.9e+00	4.0e+00	4.0e+00	4.0e+00
p-value	(1.3e-03**)	(2.5e-03**)	(8.1e-03**)	(1.7e-02*)	(1.7e-02*)	(4.2e-02*)	(1.6e-02*)	(1.6e-02*)	(1.6e-02*)	(1.6e-02*)

Table 9: Table summarizing the feature importances found for the trained weighting network with corresponding t -statistics and p -values. Significance levels: $^* \alpha = 0.05$, $^{**} \alpha = 0.01$, and $^{***} \alpha = 0.001$.

5 Discussion

In this section, we reflect on the results, and present areas for further work.

5.1 Reflections on the Results

This paper sought to investigate two hypotheses: First (1), we hypothesized that reducing the number of assumptions on input features and relationships, models, and outputs as possible could lead to well-performing forecasting algorithms and increased accuracy. Second, (2) the hypothesis that state-of-the-art machine learning methods like LSTM Autoencoders can compress, extract and represent information that it is hard for humans to capture in as many as 42 human-defined statistical features.

Hypothesis 1: Fewer assumptions lead to better results

We find our approach to out-compete other methods. The reduced assumptions in model building likely lead to an increase in accuracy, evidenced by the statistically significant OWA loss improvements and the DONUT model’s reliance on the novel Autoencoder features.

Our ensemble weighting model, built on the combination ensembling method, shows convincing results. With an OWA of 0.830 (see, Table 7) our model beats 48 participants in the competition, only outperformed by Smyl (2020), which uses an entirely different approach. We have also ran a *t*-test on the result, with H_0 being that our true mean is equal to that of Montero-Manso et al. (2020), which we reject with $p = 0.006$.

We find some evidence that adding more models to the ensemble improves results regarding the model output. For example, Figure 15 in Figure 15 show that the DONUT model’s ensemble has a mean weighting of Ornstein-Uhlenbeck and Quantile Regression with $\tau = 0.99$ is higher than some of the models already included in the FFORMA ensemble. This finding indicates that augmenting with diverse models can be beneficial. Furthermore, in 27% of cases, the weighting model uses ten or more models. Thus, in a quarter of the series of the M4 competition, the weighting model recommends a weighting that the FFORMA model could not possibly predict, given its ensemble only contains nine models.

Hypothesis 2: Machine learning methods can find features humans cannot

There seems to be evidence to support the hypothesis that machine learning methods can find efficient representations of time series features that are hard for humans.

The features extracted by the Autoencoder represent statistically different information from those of the statistical features in several cases. For example, Figure 17 shows that, together with “period,” the LSTM features are among the most detrimental to scramble for the model: in this interpretation of feature “importance,” 4 out of 5 of the most “important” features, are generated by the LSTM. Even though each scrambling amounts to a 0.004 increase in OWA, the comparison of interest is the relative importance between the LSTM features and the statistical ones. Indeed, our results indicate that the LSTM features contain information as valuable, if not more valuable than the statistical features. The fact that several models trained during the development of the DONUT approach showed reliance on many of the same LSTM features further supports the finding.

The Figure 18 graph depicts a hierarchical clustering of feature correlation in the form of a dendrogram. For example, in the figure, one can see how the dendrogram clustered some LSTM features with each other and more distantly with the statistical features (see, e.g., clusters 1 and 4 in Figure 18). This clustering might indicate that the LSTM features contain information not present in the statistical features alone. Furthermore, some of the single most “important” statistical features, like `lstm_6`, `lstm_9`, `lstm_14`, are all present in different clusters, showing high correlation distance to each other, indicating that they have also found different features that are all the while important.

Furthermore, as mentioned in Section 3.6, the Neural Net-based autoencoder functions as a Non-Linear Principal Component Analysis (NLPCA), meaning that the method can extract non-linear features and relationships. These are the features that are hard for humans and classical statistical methods to extract. In Figure 24, we present one example of this kind of feature. In this figure, one can see from the shape of the different-colored tiles that there is a non-linear relationship between the LSTM feature and the resulting forecasting OWA loss. In particular, there seems to be a relationship like $c = x^2 + y^2$, where c is a threshold between doing better and worse than its average.

Among other results, Figure 23 shows that our model outperforms Montero-Manso with statistical significance $p < 0.05$ when seasonal strength is low, but our novel lstm31 feature is positive—not falsifying that our LSTM features do not contain relevant information different from the traditional statistical features.

5.2 Further Work

There is much testing we would have done with more time. This section offers some thoughts on possible improvements for the weighting model and the Autoencoder. The relationship between the post facto optimal solution and the final prediction result could also offer appealing topics for further study.

Firstly, one can do considerable optimization of the weighting model, DONUT. We wanted to ensemble many of our fully trained models to create an ensemble of ensembles. We believe the meta ensemble would be compelling since we observed different ways of failing and utilizing the features between the weighting Neural Nets trained with slightly different hyperparameters. Alas, the time would not allow this.

Running multiple short training runs to reduce overfitting showed promising results in that some weighting models found different features more important than others. A hypothesis is that another layer of ensembling could thus zero out individual flaws given a low degree of correlation. We propose to use the top k performing neural nets on the validation set, according to a loss measure criteria (in our case, validation loss plus the absolute deviation from training loss), and then use a simple average over these identities. We find this approach analogous to that of a random forest.

We would also have liked to use feature selection to remove features that did not contribute sufficiently to the weighting model's predictive power. From Figure 17 it is evident that "lumpiness", "lstm.15" and "spike" is direct noise to the weighting entity. As such, removing these could help in the weight nets predictive power.

We also have enticing possibilities for further work on the Autoencoder. For example, we would have liked to reduce the number of features to make each dimension contain more predictive power in the embedding vector. This dimensionality reduction seems an even more attractive option after the results found in Figure 17. Indeed, many LSTM-features are not vital in the final prediction (in that their randomization causes no difference with statistical significance). Furthermore, we had ideas of making the auto-encoded features time-dependent as well. For instance, one could run the Autoencoder over series with different time deltas to produce features and then apply exponential smoothing to the output in the final feature measure. There would, of course, be no guarantee that this would produce more promising results than the current solution, but one could experiment with a decay factor of different sizes to make the features more or less short-term dependent, which is worth investigating.

We think there are more effective relationships to study between the ex post facto optimal solution and the actual predictive performance. Indeed, the ex-post facto solution offers an upper bound for the weighting entity as seen in equation Equation 21. Compared with the forecast selection ex-post facto approach, the movement of this bound could lead to some fascinating results. For example, a significant finding would be that an actual weight result outperformed the model selection approach. Furthermore, one could find areas where the relationship between model selection and model combination could be understood.

As the last point, we would have liked to train on more data and extend the model with relevant panel data. One could also add augmented data specifically aimed at increasing performance where the ensemble cannot predict well or for the specific data categories which are underrepresented. In the lines of Goodfellow et al. (2016):

"The best way to make a machine learning model generalize better is to train it on more data. Of course, in practice, the amount of data we have is limited. One way to get around this problem is to create fake data and add it to the training set."

We would also have liked to try our ensemble forecasting approach in real-world applications, such as predicting epidemic data or prices.

6 Conclusion

This paper aimed to reduce assumptions about inputs and outputs of a combination ensemble with a DONUT procedure (DO Not UTilize human assumptions). We also wanted to investigate if LSTM generated time-series features contain more crucial information than traditional statistical features. Our reduction of input assumptions through auto-generated features as part of an ensemble model that outperforms the statistical-feature-based ensemble FFOMA by Montero-Manso et al. (2020). Furthermore, we find that our weighting model uses both LSTM features and statistical features to achieve this. Minor indications point in the direction of LSTM superiority over statistical features alone. In a correlation dendrogram analysis, it is evident that LSTM features are indeed different from one another and form two clusters dissimilar from most standard statistical features. We also find that increasing output space by adding available models is something the weighting model learns to use, partly explaining the accuracy gains.

Lastly, we presented a short proof that model combination is superior to model selection a posteriori and quantified their difference through linear optimization on the M4 dataset.

Bibliography

Armstrong, J. S. & Collopy, F. (1992). Error measures for generalizing about forecasting methods: Empirical comparisons. *International journal of forecasting*, 8(1), 69–80.

Bates, J. M. & Granger, C. W. (1969). The combination of forecasts. *Journal of the Operational Research Society*, 20(4), 451–468.

Bessembinder, H., Coughenour, J. F., Seguin, P. J. & Smoller, M. M. (1995). Mean reversion in equilibrium asset prices: Evidence from the futures term structure. *The Journal of Finance*, 50(1), 361–375.

Bibbona, E., Panfilo, G. & Tavella, P. (2008). The Ornstein–Uhlenbeck process as a model of a low pass filtered white noise. *Metrologia*, 45(6), S117.

Breiman, L. (2001). Random forests. *Machine learning*, 45(1), 5–32.

Brooks, C. (2019). *Introductory Econometrics for Finance* (4th ed.). Cambridge University Press. <https://doi.org/10.1017/9781108524872>

Cauchy, A. et al. (1847). Méthode générale pour la résolution des systèmes d'équations simultanées. *Comp. Rend. Sci. Paris*, 25(1847), 536–538.

Chen, T. & Guestrin, C. (2016). Xgboost: A scalable tree boosting system. *Proceedings of the 22nd ACM SIGKDD international conference on knowledge discovery and data mining*, 785–794.

Clemen, R. T. (1989). Combining forecasts: A review and annotated bibliography. *International journal of forecasting*, 5(4), 559–583.

Fildes, R., Hibon, M., Makridakis, S. & Meade, N. (1998). Generalising about univariate forecasting methods: further empirical evidence. *International journal of Forecasting*, 14(3), 339–358.

Gauss, C. F. (1823). *Theoria combinationis observationum erroribus minimis obnoxiae* (Vol. 2). H. Dieterich.

Goodfellow, I., Bengio, Y. & Courville, A. (2016). *Deep Learning* [<http://www.deeplearningbook.org>]. MIT Press.

Greene, W. (2018). *Econometric Analysis*. Pearson.

Hornik, K., Stinchcombe, M. & White, H. (1989). Multilayer feedforward networks are universal approximators. *Neural networks*, 2(5), 359–366.

Hyndman, R. J. & Athanasopoulos, G. (2018). *Forecasting: principles and practice*. OTexts.

Koenker, R. & Bassett Jr, G. (1978). Regression quantiles. *Econometrica: journal of the Econometric Society*, 33–50.

Kramer, M. A. (1991). Nonlinear principal component analysis using autoassociative neural networks. *AIChE journal*, 37(2), 233–243.

Kwiatkowski, D., Phillips, P. C., Schmidt, P. & Shin, Y. (1992). Testing the null hypothesis of stationarity against the alternative of a unit root: How sure are we that economic time series have a unit root? *Journal of econometrics*, 54(1-3), 159–178.

Laptev, N., Yosinski, J., Li, L. E. & Smyl, S. (2017). Time-series extreme event forecasting with neural networks at uber. *International conference on machine learning*, 34, 1–5.

Lemke, C. & Gabrys, B. (2010). Meta-learning for time series forecasting and forecast combination. *Neurocomputing*, 73(10-12), 2006–2016.

Li, L., Jamieson, K., DeSalvo, G., Rostamizadeh, A. & Talwalkar, A. (2017). Hyperband: A novel bandit-based approach to hyperparameter optimization. *The Journal of Machine Learning Research*, 18(1), 6765–6816.

Makridakis, S., Andersen, A., Carbone, R., Fildes, R., Hibon, M., Lewandowski, R., Newton, J., Parzen, E. & Winkler, R. (1982). The accuracy of extrapolation (time series) methods: Results of a forecasting competition. *Journal of forecasting*, 1(2), 111–153.

Makridakis, S., Chatfield, C., Hibon, M., Lawrence, M., Mills, T., Ord, K. & Simmons, L. F. (1993). The M2-competition: A real-time judgmentally based forecasting study. *International Journal of forecasting*, 9(1), 5–22.

Makridakis, S. & Hibon, M. (2000). The M3-Competition: results, conclusions and implications. *International journal of forecasting*, 16(4), 451–476.

Makridakis, S., Spiliotis, E. & Assimakopoulos, V. (2018). The M4 Competition: Results, findings, conclusion and way forward. *International Journal of Forecasting*, 34(4), 802–808. <https://doi.org/https://doi.org/10.1016/j.ijforecast.2018.06.001>

Makridakis, S., Spiliotis, E. & Assimakopoulos, V. (2020). Predicting/hypothesizing the findings of the M4 Competition. *International Journal of Forecasting*, 36(1), 29–36.

Minsky, M. & Papert, S. A. (2017). *Perceptrons: An introduction to computational geometry*. MIT press.

Montero-Manso, P., Athanasopoulos, G., Hyndman, R. J. & Talagala, T. S. (2020). FFORMA: Feature-based forecast model averaging. *International Journal of Forecasting*, 36(1), 86–92.

Newbold, P. & Granger, C. W. (1974). Experience with forecasting univariate time series and the combination of forecasts. *Journal of the Royal Statistical Society: Series A (General)*, 137(2), 131–146.

Ng, E., Wang, Z., Chen, H., Yang, S. & Smyl, S. (2020). Orbit: Probabilistic Forecast with Exponential Smoothing. *arXiv preprint arXiv:2004.08492*.

Petropoulos, F., Apiletti, D., Assimakopoulos, V., Babai, M. Z., Barrow, D. K., Taieb, S. B., Bergmeir, C., Bessa, R. J., Bijak, J., Boylan, J. E. et al. (2020). Forecasting: theory and practice. *arXiv preprint arXiv:2012.03854*.

Reed, R. & MarksII, R. J. (1999). *Neural smithing: supervised learning in feedforward artificial neural networks*. Mit Press.

Reid, D. J. (1969). *A comparative study of time series prediction techniques on economic data*. University of Nottingham, Library Photographic Unit.

Schöbel, R. & Zhu, J. (1999). Stochastic volatility with an Ornstein–Uhlenbeck process: an extension. *Review of Finance*, 3(1), 23–46.

Siregar, B., Butar-Butar, I., Rahmat, R., Andayani, U. & Fahmi, F. (2017). Comparison of exponential smoothing methods in forecasting palm oil real production. *Journal of Physics: Conference Series*, 801(1), 012004.

Smyl, S. (2020). A hybrid method of exponential smoothing and recurrent neural networks for time series forecasting. *International Journal of Forecasting*, 36(1), 75–85.

Snoek, J., Larochelle, H. & Adams, R. P. (2012). Practical bayesian optimization of machine learning algorithms. *Advances in neural information processing systems*, 25.

Student. (1908). The probable error of a mean. *Biometrika*, 1–25.

Timmermann, A. (2006). Forecast combinations. *Handbook of economic forecasting*, 1, 135–196.

Wiener, N. (1976). Collected Works, Vol. 1, P. Masani.

Wolpert, D. H. (1996). The lack of a priori distinctions between learning algorithms. *Neural computation*, 8(7), 1341–1390.

Appendix

A Analysis of the Inner Workings of the LSTM Autoencoder

Furthermore, we conducted studies into the embeddings themselves to see if they contain any information of value. Again, a synthetic data-set was constructed, see Figure 25. From the right, we can see that the linear lines, sines, and Taylor approximations look very similar to each other with the level of noise added. Multiple, different series of this type was fed to the encoder an encoder of the same type, but with a smaller embedding of 4, to produce embedding vectors.

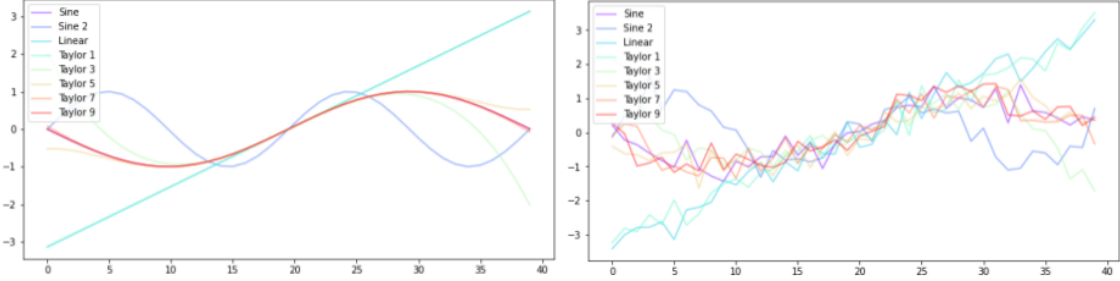


Figure 25: Synthetic data-set created to test noise filtering and clustering on increasingly difficult examples. The data is comprised of several copies of two different sines with different frequencies, and several Taylor approximations to one of them. All have considerable random noise added to them.

In Figure 26, the projection of this 4-dimensional space down onto each of the two-dimensional planes is shown. The colors code what time-series produced the dot. At first glance, one sees that the different-colored dots are well-separated. Furthermore, one can observe that different planes place the groups differently in spatial relationship to each other. E.g. in the second panel showing dimensions 0 and 2, the dots "move" up and to the left when the frequency increases, and $\sin x$ and $\sin 2x$ are very close to each other. On the other hand, on the fourth panel showing dimensions 1 and 2, all clusters are spread around the edges, and $\sin x$ and $\sin 2x$ are on opposite ends. This hints that different dimensions captures different aspects of a time-series.

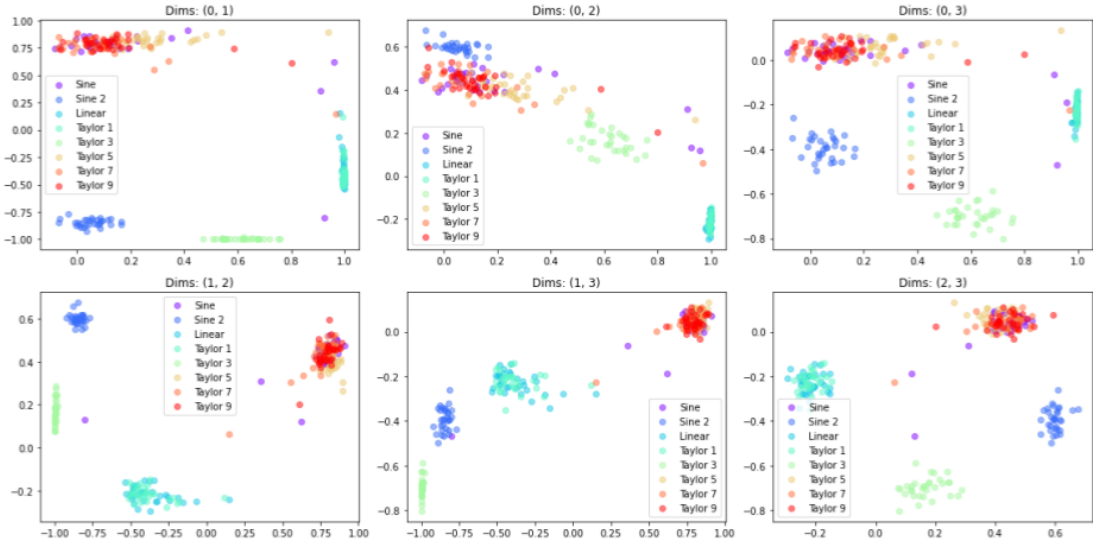


Figure 26: The six ways to slice the 4-dimensional space of one version of the trained autoencoder. The network is trained on M4 data, and the encoder is given the sines and Taylor approximations, and the raw outputs are plotted.

B The M4 Competition Dataset of 100 000 Time Series

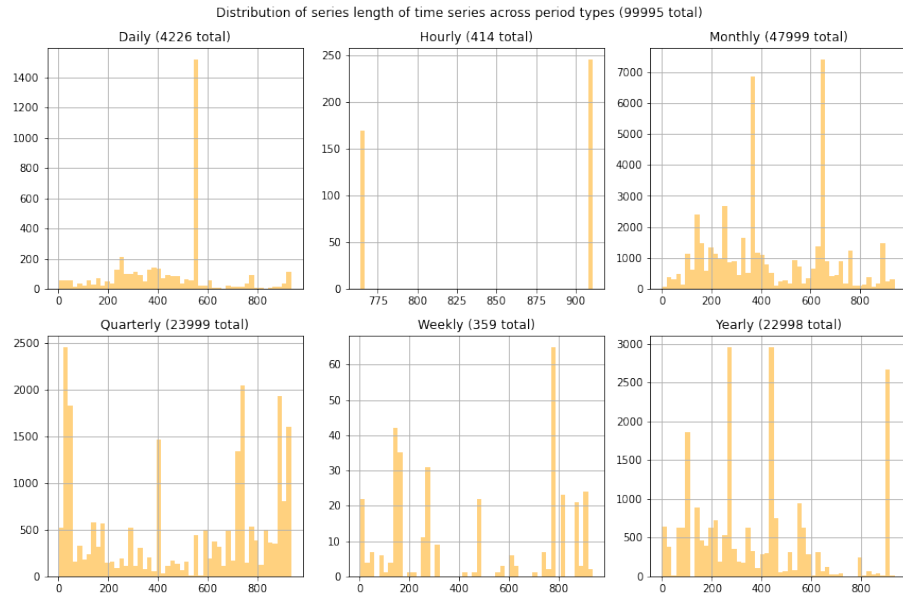


Figure 27: The distribution of different series lengths per series periodicity.

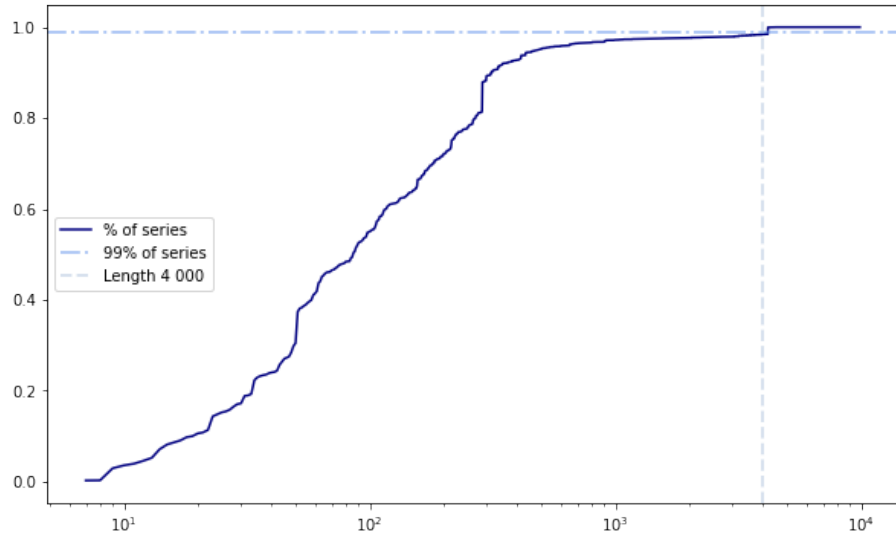


Figure 28: Cumulative number of time-series for series with for length to the value or shorter. By limiting the longest time-series to be 4 000, one in effect truncates less than 1% of all time-series, but saves more than half the storage space in memory while working with the data.

C Feature and Loss Heat-maps

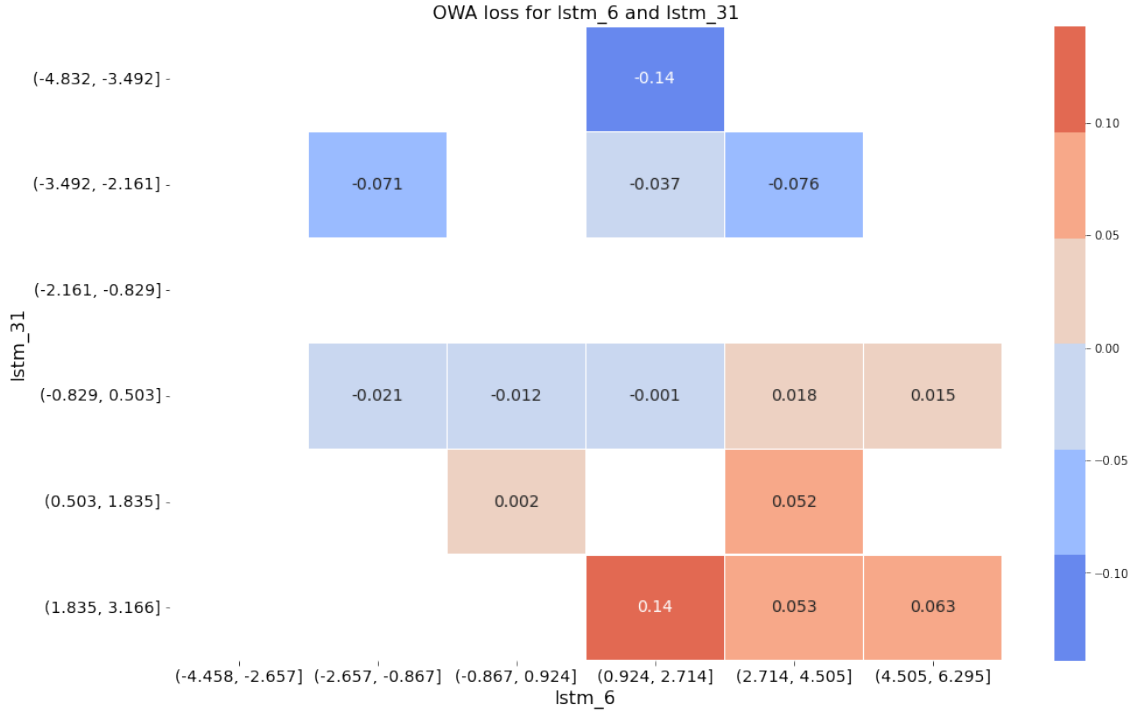


Figure 29: $p - value < 0.05$: When both lstm_31 and lstm_6 is low, or model beats Montero-Manso et al. (2020) by a significant margin. A decreasing linear combination between the two features seems to be positive for our weight nets predictive power.

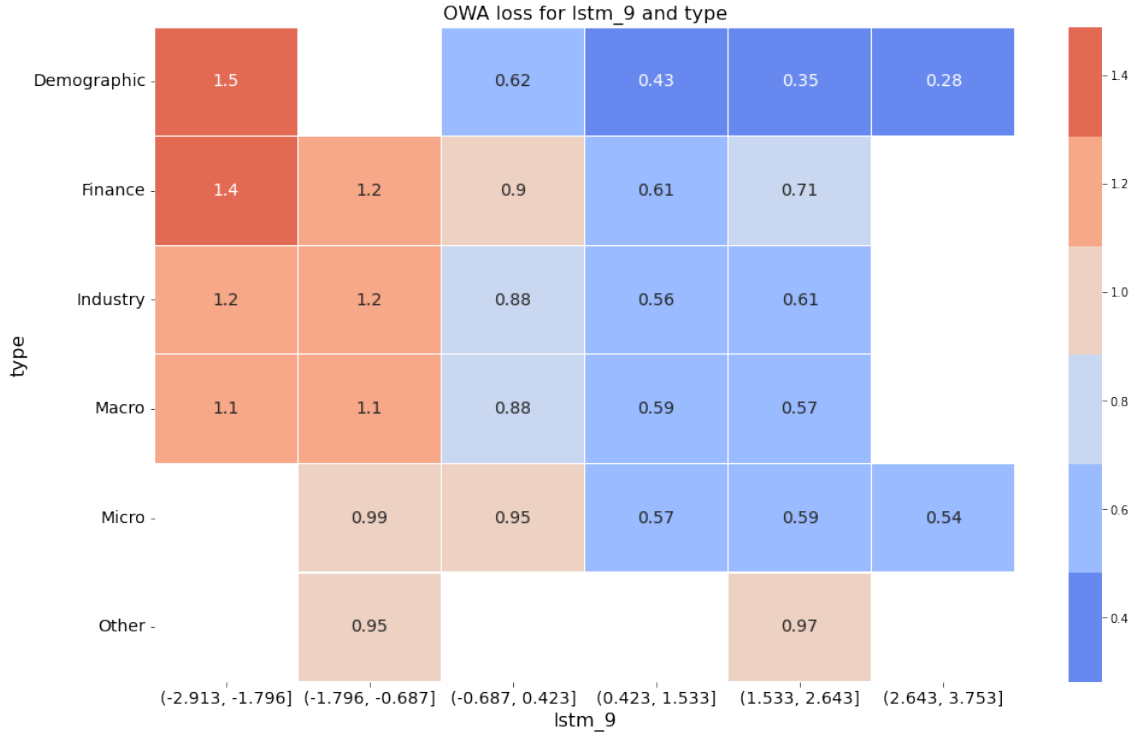


Figure 30: $p - value < 0.05$: lstm_9 also shows a clear tendency of reducing error, over all types.

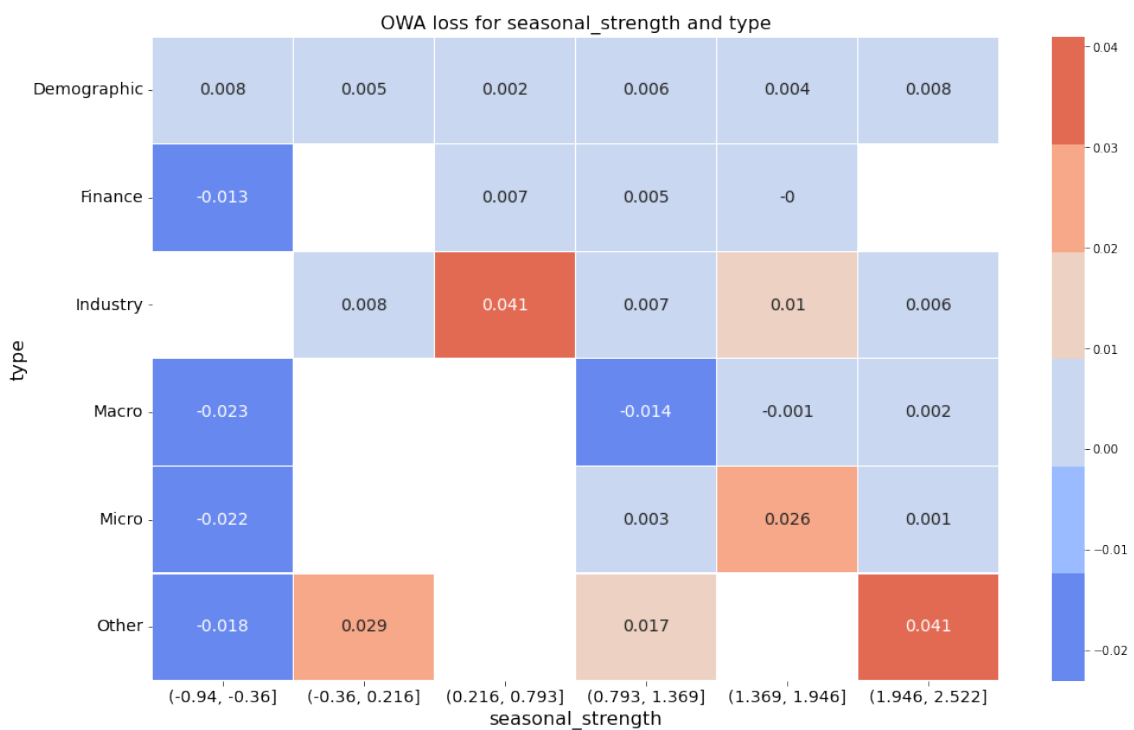


Figure 31: $p - value < 0.05$: Shows that when seasonality is low, has a decreased loss compared to Montero-Manso et al. (2020) by around .02 OWA. Such a loss reduction over all series is enough to move from a second to 6th place in the m4 competition.